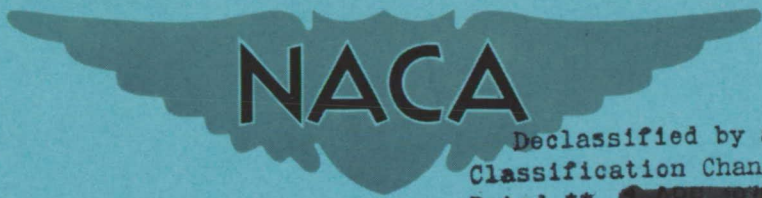


X 62 63997

Copy 354

~~CONFIDENTIAL~~

RM A56G24



Declassified by authority of NASA
Classification Change Notices No. _____
Dated ** JUN 30 1971

213

RESEARCH MEMORANDUM

AN AIRBORNE SIMULATOR INVESTIGATION OF THE ACCURACY OF
AN OPTICAL TRACK COMMAND MISSILE GUIDANCE SYSTEM

By Joseph G. Douvillier, Jr., John V. Foster,
and Fred J. Drinkwater III

Ames Aeronautical Laboratory
Moffett Field, Calif.

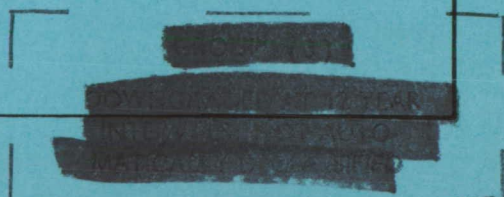
~~CATEGORY~~
~~SPECIAL HANDLING~~
7

~~CLASSIFIED DOCUMENT~~

~~This material contains information affecting the National Defense of the United States within the meaning of the espionage laws, Title 18, U.S.C., Secs. 793 and 794, the transmission or revelation of which in any manner to an unauthorized person is prohibited by law.~~

NATIONAL ADVISORY COMMITTEE FOR AERONAUTICS

WASHINGTON
November 23, 1956



~~CONFIDENTIAL~~



NATIONAL ADVISORY COMMITTEE FOR AERONAUTICS

RESEARCH MEMORANDUM

AN AIRBORNE SIMULATOR INVESTIGATION OF THE ACCURACY OF
AN OPTICAL TRACK COMMAND MISSILE GUIDANCE SYSTEM

By Joseph G. Douvillier, Jr., John V. Foster,
and Fred J. Drinkwater III

SUMMARY

An airborne missile simulator was used to represent visually the predicted flight behavior of the Navy XASM-N-7 Bullpup air-to-surface missile, which is guided along the line of sight to the target by "bang-bang" radio signals controlled by the pilot of the launch airplane. The accuracy with which this missile (insofar as represented by the simulator) can be guided was assessed in simulated attack runs against a ground test target. Runs were made for firing ranges of 15,000 feet and 8,000 feet, with and without initial missile dispersion, at a nominal attacker indicated airspeed of 350 knots and dive angle of 20°. Five pilots with varying degrees of related experience participated in the tests.

Quantitative response measurements showed that the simulator gave a good representation of the trajectory and control characteristics predicted for the Bullpup missile, and the simulation appeared plausible to the pilots. With no initial dispersion, the probable miss distance was 29 feet for the 15,000-foot firing range runs and 20 feet for the 8,000-foot firings. Initial dispersion caused no significant increase in the probable miss distance. There was no evidence of marked differences in guidance proficiency among the test pilots; a moderate number of simulated firing runs was required to attain reasonably constant proficiency; and there was no evidence of appreciable loss in proficiency after a pilot layoff of as long as 1 month.

INTRODUCTION

The Air Force and the Navy have recently expressed interest in air-launched missiles with simple guidance systems of the type diagrammed in figure 1. The missile would be guided along the visual line of sight to the target by radio signals controlled by the pilot of the launch airplane.



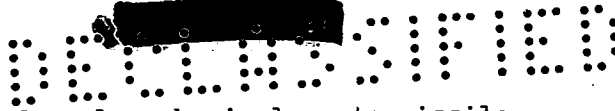
The Navy XASM-N-7 Bullpup is one such missile under development. At a meeting held during early developmental stages, representatives of the Navy, the contractor, and the Ames Aeronautical Laboratory discussed the use of simulators for predicting the miss-distance statistics of the missile with the original or with modified guidance systems. It was recognized that studies using ground simulators, proposed by the Navy and the contractor, were essential for preliminary investigation. Although ground simulators are conceivable which can represent to some extent the simultaneous airplane and missile control tasks, for simplicity the proposed ground studies involved only the missile control task. Thus, the adequacy of this type of simulation for predicting quantitatively the accuracy obtainable with the actual weapon seemed questionable. Accordingly, Ames personnel suggested an airborne missile simulator which the pilot would control while simultaneously flying the launch airplane.

Such a simulator, based on principles and components utilized previously in an airborne target simulator (ref. 1), was developed at Ames Aeronautical Laboratory. The missile is represented by a collimated dot of light (focused at infinity and hence free of parallax) projected onto the windshield of the launch airplane. The position of this dot is established by line-of-sight information from a missile analog computer and a space reference system. The pilot attempts to maintain the simulated missile on the line of sight to an actual target. For the present program, characteristics of the command switch and the missile analog computer were made to represent those of the originally proposed off-on, or "bang-bang," acceleration-control system for the XASM-N-7 missile.

A number of simulated missile attacks were made, under typical launching conditions, against a ground test target. Five pilots with varying degrees of experience in this control task participated in the tests. The miss distance for each run was evaluated from photographic records; and statistical quantities, such as standard deviation, bias, and circular probable error, were computed for the various test conditions. The airborne missile simulator and the results of the test program are described in the present report.

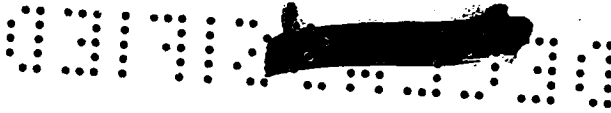
NOTATION

- A acceleration parallel to flight path, ft/sec²
- a acceleration normal to flight path (approximately normal to IS_M), ft/sec²
- AL "antenna" axis
- CPE circular probable error, the value of miss angle corresponding to $P = 50$ percent, milliradians



LS_M	line of sight from launch airplane to missile
$\angle LS_M$	angle between LS_M and a reference fixed in space (fig. 21)
$\dot{\angle LS_M}$	angular rate of rotation of LS_M in space
LS_T	line of sight from launch airplane to target
$\angle LS_T$	angle between LS_T and a reference fixed in space (fig. 21)
ML	optical gunsight mirror axis
P	the probability that a single, experimental value of miss angle will be less than a given value, percent
R	instantaneous value of range from launch airplane to missile, ft
RL	launch airplane reference line
r	radial miss angle measured from the point (\bar{x}, \bar{y}) , $\sqrt{(x-\bar{x})^2 + (y-\bar{y})^2}$, milliradians
r_T	radial miss angle measured from test target center, $\sqrt{x^2 + y^2}$, milliradians
V	velocity parallel to flight path, ft/sec
v	velocity normal to LS_M , ft/sec
x	azimuth miss angle, measured from test target center, positive to the right of target center, negative to the left, milliradians
\bar{x}	mean value of x, milliradians
y	elevation miss angle, measured from test target center, positive above target center, negative below, milliradians
\bar{y}	mean value of y, milliradians
γ	angle between flight path and a fixed space reference (fig. 21)
ϵ_{LS}	instantaneous value of angle between LS_M and LS_T
ϵ_r	circular probable error with respect to the point (\bar{x}, \bar{y}) , milliradians
ϵ_{r_T}	circular probable error with respect to target center, milliradians





η	available missile maneuvering load factor, g units
σ_x	standard deviation of the azimuth miss angle distribution, milliradians
σ_y	standard deviation of the elevation miss angle distribution, milliradians
ϕ	angle between LS_M and missile flight path
ψ	angle between LS_M and airplane flight path

Subscripts

A	launch airplane
M	missile
o	time of firing

APPARATUS

Missile Simulator

A perspective of the missile-target-launch airplane relationship is shown in figure 1. The pilot views directly both the missile and the ground target. To maintain the missile along the line of sight to the target he commands "full on-full off" missile acceleration, in azimuth and in elevation, either separately or simultaneously. These acceleration commands are applied through a thumb-operated, eight-position, spring-return toggle switch on the airplane control stick grip, and are transmitted as radio signals to a simple bang-bang type missile servo system. The resulting control surface deflection drives the missile in the desired direction.

Following is a brief description of the airborne missile simulator used in the present tests. A more detailed description is given in Appendix A. The airborne target simulator described in reference 1 was modified for use as a missile simulator (fig. 2) in which the pilot's command signal is applied to a missile analog computer. Output of the computer is an analog of the rate of rotation in space of the line of sight to the missile, LS_M . A space-stabilized axis, which represents LS_M , is precessed according to the varying output signal from the computer, and its angular position in space is displayed to the pilot as a collimated dot projected onto the windshield of the launch airplane. The gain of the





analog computer is programmed as a continuous function of missile time of flight, so that the output varies as the predicted available missile load factor and inversely as missile range. For these tests the computer was adjusted to simulate the predicted response characteristics of the Navy XASM-N-7 Bullpup missile. Time histories of available maneuvering load factor and of range were obtained from the missile contractor and are shown in figure 3. The simulated effects of gravity and, optionally, initial dispersion are provided by appropriate electrical inputs to the computer. A modified radar antenna and antenna drive circuit from an E-3 fire-control system provide the space-stabilized axis. The dish and dipole were removed so that the "antenna" consists of only the two (azimuth and elevation) type HIGU integrating rate-gyro units and the antenna gim-bals. The windshield display is effected through a modified A-4 gunsight head, the mirror drive of which is essentially slaved to the antenna.

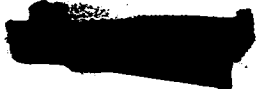
INSTALLATION IN TEST AIRPLANE

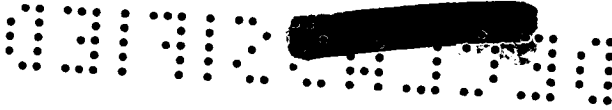
A photograph of the TV-1 test airplane is presented in figure 4. Some modifications of the airplane nose section and the cockpit and instrument panel arrangements were necessary to accommodate simulator equipment.

The antenna assembly (whose axis represents line of sight to the missile), including the two HIGU gyros, and most of the electronic components of the simulator are shown in figure 5. The camera mounted in the nose was not used for these tests.

Figure 6 is a photograph of the A-4 gunsight head (ref. 2) used for the windshield display, installed in the test airplane. Only the mirror drive and caging assembly, the reticle assembly, and mechanical components of the range assembly are used. Removed from the sight head were the target wing-span setting lever and associated linkage, and the electrical components of the range assembly. Figure 7 is a photograph of the illuminated reticle (the missile dot and the adjustable range ring) projected onto the windshield of the test airplane. The range ring diameter adjusting knob and index dial are shown in figure 6. When the simulator master switch is closed, the reticle is always illuminated, except for the 1 second immediately after firing and for a brief period following the completion of a run. Before firing, the reticle is locked in alignment with the airplane reference line and used as a fixed gunsight when the pilot sets up a firing run.

The pilot's simulator controls are pointed out in figure 8. Through the three-position camera and instrument switch, the pilot elects whether data are recorded by the sight head camera, both the camera and the nine-channel oscillograph, or neither. The missile is fired with a trigger switch on the control-stick grip. After firing, and before impact is





signalled by a disappearance of the reticle, control of the simulated missile is effected through manipulation of the command switch. Detents of the switch are so fashioned that a command change from one direction (switch position) to another can be made without passing through neutral. The sense of the commanded acceleration signal coincides, in both azimuth and elevation, with the direction of displacement of the command switch handle (fig. 8). Space-stabilization performance of the antenna-mirror-drive system can be checked when the stabilization check switch is opened, thereby removing the input to the drive system.

TEST TARGET

The target shape sketched in figure 9 was painted in white on an unused asphalt runway. For test flights, the diameter of the sight head range ring (fig. 7) was adjusted to subtend a visual angle equal to the angle subtended by the distance between the range marks at the preselected firing range. The dive-angle marks were used to read from the data film the instantaneous dive angle during a test run.

INSTRUMENTATION

During a test run, 35mm color motion pictures of the test target and the superposed sight head reticle were taken continuously, at ten frames per second, by the data-recording camera. The camera, mount, and mirror are shown in figure 6. The mirror was small enough not to obscure significantly the pilot's view. After installation, the camera was calibrated, so that the angle between LS_M and LS_T could be determined from the data film (of which a sample is shown in fig. 10).

A standard miniature NACA nine-channel oscillograph, pointed out in figure 5, was used to record the quantities indicated on the sample oscillograph film record presented in figure 11. Oscillograph records were used primarily to monitor the performance of the simulator.

TESTS AND RESULTS

Simulator Performance Checks

The performance of the simulator was checked on the ground before installation in the test airplane. In addition, on every test flight a check of the space-stabilization system was made and recorded on the 35mm data film. Details of these tests are given in Appendixes A and B.





Simulated Attacks on Test Target

Test procedure.- Since preliminary investigation of the Bullpup missile-guidance problem by the Navy and the contractor shows that launch airplane dive angle and airspeed have no marked effect on guidance accuracy, all Ames tests were run at one set of airplane trim conditions: 20° dive angle, 350 knots indicated airspeed. Data were obtained from 15,000- and 8,000-foot firing ranges, the maximum and minimum predicted practical values for the Bullpup.

To execute a firing run the pilot established the selected airplane trim conditions while beyond the firing range, using the reticle as a fixed gunsight to track the ground test target. When the preset ranging diameter appeared equal to the distance between target range marks (fig. 9), the pilot fired the simulated missile. The reticle immediately disappeared. When no initial dispersion was added, the reticle reappeared 1 second later, about on the extension of the airplane reference line, with the simulated line of sight to the missile stabilized in space, the line-of-sight rate of rotation equal to zero, and the simulated missile acceleration equal to gravity. When initial dispersion was added, the reticle appeared 1 second after firing, displaced at random about 4° from the airplane reference line, with a velocity directed toward the airplane reference line and proportional to the angle between the line of sight and the reference line. It is believed that 4° is representative of the more severe values of dispersion to be encountered with the actual missile.

When the reticle reappeared after firing, the pilot attempted to maintain the missile dot along the line of sight to the target, LS_T , by applying available acceleration commands with the thumb-operated command switch. Throughout the run the test airplane was maintained in a 20° dive at 350 knots. Impact of "missile" and target (10.8 seconds after firing for the 15,000-foot runs, 5.5 seconds for the 8,000-foot runs) was signalled to the pilot by a final disappearance of the reticle. Fifteen seconds after firing, the reticle reappeared in a locked position; and the simulator was ready to be fired again.

The first group of test firings was made with no initial dispersion, from both 15,000- and 8,000-foot firing ranges. Initial dispersion was added and the tests repeated. Pilot C flew only 15,000-foot, no dispersion runs; pilots D and E made 15,000- and 8,000-foot, no dispersion runs; only pilots A and B made runs for all launch conditions.

Pilots A, B, and C had considerable previous experience in optical tracking tasks and had flown the Ames airborne target simulator described in reference 1. Pilot D had some experience with a Bullpup missile ground simulator built by the contractor; and pilot E had considerable flight experience with an airborne Bullpup simulator constructed by the Naval Air Development Center.



Data reduction.- The data were read from the 35mm film (fig. 10) on a Telereadex Type 29a automatic film reading machine. Azimuth miss angle, x , was read according to the horizontal displacement of the missile dot from the target center; elevation miss angle, y , according to vertical displacement. Radial miss angle with respect to the target was calculated from the formula:

$$r_T = \sqrt{x^2 + y^2}$$

Miss data were obtained for each firing run from the frame of the data film immediately before impact (reticle light extinguished). In addition, for several of the 15,000-foot firing range runs, both with and without dispersion, miss data were interpolated at four points intermediate between firing and impact.

In order to assure that actual test-flight conditions approximated nominal values, occasional readings of airplane dive angle and range to target were taken from the data film according to the known geometric relationship among the test target dive angle and range marks (fig. 9), and the calibration of the 35mm camera.

Presented in tables I through IV are the impact miss data for each run. Since the error observed by the pilot is fundamentally angular, miss data are expressed in angular measure rather than in linear measure. A nominal value of linear miss, in feet, can be calculated by multiplying the angular miss by 8.6 for the 15,000-foot firing range runs, and by 4.7 for the 8,000-foot firings.

It should not be construed from the absence (in tables I through IV) of miss data for several runs that large values of miss angle have been ignored. On the contrary, values of radial miss larger than 20 milliradians were never encountered. Absence of data implies, generally, that the run was intended for purposes other than the recording of miss data against the test target (e.g., space-stabilization check).

To determine \bar{x} and \bar{y} , the mean azimuth and elevation miss angles, the cumulative probability, P , of x and of y for each launch condition was plotted on normal probability graph paper (refs. 3 and 4); P of a given value of miss angle is the probability that a single value of miss angle will be less than the given value. Mean value of miss angle is that value for which P is 50 percent. The standard deviation, σ , a measure of the dispersion of the miss angle distribution, is taken as the change in ordinate of the cumulative probability curve between $P = 50$ percent and $P = 84.1$ percent. Figures 12 through 15 show the cumulative probability curves of x and y for all four firing conditions; \bar{x} , \bar{y} , σ_x , and σ_y are noted on each figure.



The radial miss angle, r , about the mean point of impact (m.p.i.), listed in tables I through IV was calculated from the formula:

$$r = \sqrt{(x - \bar{x})^2 + (y - \bar{y})^2}$$

where (\bar{x}, \bar{y}) defines the m.p.i.

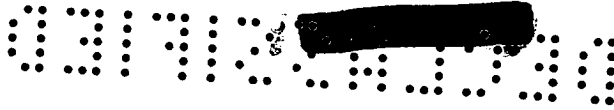
Cumulative probability curves of \sqrt{r} and $\sqrt{r_T}$ for all four launch conditions are presented in figures 16 through 19. It was found that if the square roots are plotted, instead of the values themselves, the curve is a straight line. The circular probable error, ϵ_r centered at the m.p.i., or ϵ_{r_T} centered at the target, is the square of the value of \sqrt{r} or of $\sqrt{r_T}$ corresponding to $P = 50$ percent.

Interpolated values of (angular) ϵ_{r_T} , for four points intermediate between firing and impact, from several of the 15,000-foot runs are plotted in figure 20. Impact values of ϵ_{r_T} from these runs and from the 8,000-foot runs are also plotted. To obtain the intermediate range data, values of ϵ_{r_T} were interpolated from the data film at 5.5, 6.7, 7.8, and 9.3 seconds after firing for 68 of the 15,000-foot runs with no dispersion and all 47 of the 15,000-foot runs with initial dispersion. Then, each of these "times after firing" was regarded as total missile flight time (elapsed time from firing until impact); and, for each "time after firing," corresponding values of airplane-to-target range at firing and at impact were calculated according to the test programmed speeds of the missile and the launch airplane. Scales of the calculated values of firing and impact range are marked off in figure 20. The curve of linear ϵ_{r_T} as a function of time after firing, also presented in the figure, was determined by multiplying values from the faired (solid) curve of angular ϵ_{r_T} by coincident values from the impact range scale. To determine, to an acceptable degree of satisfaction, that the shape of the curve of the variation of angular ϵ_{r_T} with time is at least approximately true, 95-percent confidence limits based on the faired curve were computed, using the methods of reference 3. These limits are indicated in the figure.

Table V is a recapitulation of the statistical quantities associated with each of the test launch conditions.

In table VI is listed the ϵ_{r_T} scored by each pilot, for the various launch conditions.





Simulated Attacks on Typical Military Targets

Several impromptu attacks on typical military targets (ships, trucks, bridges, other airplanes) were made and recorded with the sight-head camera. Since the data from these runs were insufficient and the test conditions variable, no quantitative results are reported. However, pilots' comments on and opinions of simulated missile performance were obtained. Records from several of these runs have been compiled into NACA Ames film No. A-60 "Miscellaneous Firings of Airborne Missile Simulator," which is available for loan from the Ames Aeronautical Laboratory.

DISCUSSION


Simulator Performance Checks

Ground tests of simulator performance, particularly of dynamic response, showed that the final configuration represented adequately (within the pilot's threshold of perception) the predicted characteristics of the Navy XASM-N-7 missile. In addition, in-flight checks of the space-stabilization system, made during each test flight, showed excellent performance of the antenna-mirror-drive circuit. These results are discussed further in Appendixes A (ground checks) and B (in-flight checks).

Simulated Attacks on Test Target

In order to assess the effects of firing-range and missile dispersion on mean value of miss, on standard deviation, and on circular probable error, the test data (figs. 12 through 20, tables I through VI) were examined according to statistical methods outlined in references 3 and 4. The results are discussed in the following paragraphs. Also discussed are the interpolated intermediate range data read from the 15,000-foot firing-range runs; the variations in proficiency among test pilots; and, qualitatively, the effects of learning on circular probable error.

Effect of launch condition on mean values of azimuth and elevation miss angles, \bar{x} and \bar{y} .- It can be seen from table V that for all launch conditions \bar{x} was very nearly zero, a result which might have been expected since no biased azimuth disturbance (e.g., due to cross wind) was simulated. The small variations from zero, in all cases less than 1 milliradian, are reasonably ascribable to chance. The rather large value of \bar{x} for the 15,000-foot firings with initial dispersion may be associated with the relatively wide scatter (of unknown origin) in the data for that launch condition (fig. 13).



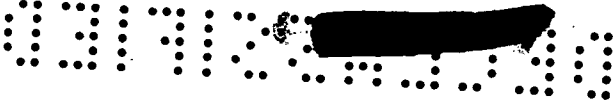
The mean elevation miss angle, \bar{y} , varied between about 1.5 and 2.5 milliradians (table V), depending on launch condition. These values are large enough to be meaningfully different from zero. The data records show that the pilots compensated for the effect of gravity with a series of pulsed, upward acceleration commands, applied so that the missile was driven above the target a greater distance than it was allowed to drop below. During a run, then, the missile was more often above than below the target, and a positively biased mean elevation error (\bar{y}) resulted.

The effect of firing-range change, or more precisely the absence of effect, on mean azimuth miss and on mean elevation miss can be seen in table V. As discussed previously, \bar{x} is essentially zero regardless of launch condition. The 0.4-milliradian increase in \bar{y} with decrease in range, for the firings both with and without initial dispersion, is of little importance.

Although, as we have seen, addition of initial dispersion had no effect on \bar{x} , curiously it resulted in a decrease in \bar{y} , from an average of about 2.2 milliradians for the firings with no dispersion to 1.4 milliradians for the firings with dispersion added. This rather surprising relationship between initial dispersion and \bar{y} may be a result of the large initial azimuth errors associated with initial dispersion, which forced the pilot to divide his attention more nearly equally between azimuth and elevation control than for the no-dispersion case (where in several runs the pilot found it wholly unnecessary to apply azimuth control), in which he could devote almost all his attention to overcompensating for gravity acceleration. (The tendency for the pilots to overcompensate for gravity is discussed in a preceding paragraph.)

Effect of launch condition on the standard deviations of the azimuth and elevation miss angles, σ_x and σ_y . For like initial dispersion conditions the data of table V show, in general, larger values of σ_x and σ_y for the 8,000-foot firing range than for the 15,000-foot range. In no instance, however, was the difference more than 1 milliradian. It is likely that the larger values of standard deviation are related to the decreased time for control of the missile, which accompanies decreased firing range.

Values of σ_x , listed in table V, show no appreciable change with initial dispersion. However, the data indicate an increase in σ_y , of about 1 milliradian, when dispersion was added. The explanation suggested for the decrease in \bar{y} with dispersion is applicable also to the increase in σ_y . With no dispersion the pilot concentrated on correcting gravity drop, to the relative neglect of the smaller azimuth errors and, hence, held σ_y less than σ_x . The introduction of large initial errors in azimuth forced the pilot to divide his attention more nearly equally between elevation and azimuth, in order to keep the azimuth error reasonably low; consequently σ_y increased, to a value about equal to σ_x .




Effect of launch condition on circular probable error (CPE), ϵ_r and ϵ_{r_T} .- Before discussing the experimental values of CPE (figs. 16 through 19 and table V), it may be well to examine briefly the statistical concept of the term. Strictly speaking, "circular probable error" applies only to a two-dimensional normal probability distribution which is truly circular; that is, which is made up of two independent one-dimensional, normal probability distributions with equal standard deviations ($\sigma_x = \sigma_y$). Moreover, the CPE should be taken about the geometric center of the circular distribution (the mean point of impact). (See ref. 4, ch. XI.)

It is obvious from table V that, in general, the experimental values of σ_x and σ_y for a given launch condition were unequal; and hence, the composite two-dimensional miss-angle distribution was elliptical, not circular. However, in reducing the experimental data the concept of CPE as the radius of a circle was retained. In order to avoid errors which might result from the use of mathematical formulas strictly applicable only to circular distributions (particularly, CPE = 0.94 times mean radial miss, ref. 4), values of circular probable error were read directly from the cumulative probability curves, figures 16 through 19. Each CPE thus read represents the radius of a circle enclosing exactly 50 percent of the experimental values of miss for the particular launch condition. As mentioned previously, two values of CPE are given for each launch condition: ϵ_r , the radius of a circle centered at the mean point of impact; and ϵ_{r_T} , centered at the target.

Values of ϵ_r and ϵ_{r_T} , noted on each of figures 16 through 19, are summarized in table V in both linear and angular measure. The largest linear value of ϵ_{r_T} , 29 feet from the 15,000-foot no-dispersion runs, is within the 30-foot CPE originally specified by the Navy for the XASM-N-7 missile.

One can observe from table V that the values of angular CPE increase with decrease in firing range, ϵ_{r_T} more markedly than ϵ_r . Variations with initial dispersion were slight in all cases; the maximum increase was about 0.5 milliradian, in ϵ_r for the 8,000-foot firings. The changes in CPE reflect changes in the respective values of mean azimuth and elevation angles, as well as in the standard deviations. It is obvious also, from table V, that though angular values of CPE were greater for the shorter firing range, the values of linear miss were smaller. This, of course, is a result of the shorter range at impact for the 8,000-foot runs - 4,700 feet, compared to 8,600 feet for the 15,000-foot runs.

Intermediate range data, interpolated CPE.- There was, as shown in table V, a change of approximately 30 percent in the linear values of ϵ_{r_T} with change in firing range from 15,000 to 8,000 feet (the extremes of firing range specified for the Bullpup). This relatively large increase in miss distance prompted the inspection of several of the 15,000-foot



runs at intermediate points between firing and impact; it was felt that some idea of at least the manner of variation of miss distance with firing range (or missile flight time) would be of operational interest. Accordingly, the interpolated values of ϵ_{r_T} which are plotted in figure 20 were determined (as previously explained) at four points between firing and impact from several of the 15,000-foot runs. For the purposes of discussion the abscissa of figure 20, time after firing, may be regarded as missile flight time (or control time). Values of ϵ_{r_T} at impact from the 8,000-foot runs (5.5 seconds flight time) were included in figure 20 to verify the order of magnitude of the interpolated values, from which the shape of the curve was inferred. It can be seen from the figure that the values at impact from the 8,000-foot runs agree, in general, with the values at 5.5 seconds after firing from the 15,000-foot runs. The relatively large discrepancy in the CPE at 5.5 seconds of the 15,000-foot dispersion runs is probably due, at least partially, to the scatter in the data for that launch condition (fig. 13).

The curve of angular CPE as a function of time after firing (fig. 20) indicates that, as missile flight time increased beyond 5.5 seconds, ϵ_{r_T} at first decreased, reached a minimum at about 8.5 seconds in this case, then increased. It might have been expected that angular ϵ_{r_T} would decrease as time for controlling the missile increased up to a point, beyond which ϵ_{r_T} would remain essentially constant. The increasing values at the longer flight times were probably due, at least in part, to a combination of the decrease in angular acceleration of the line of sight to the missile (LS_M) in response to command signals (η); the decrease, with increased range, of the visual angle subtended by the target; and the fact that, since it subtended a constant visual angle, the missile dot obscured a larger part of the ground target at the longer ranges. The latter effect, of course, would not be present with the actual missile.

It is also apparent from figure 20 that as ϵ_{r_T} in angular measure increased with decrease in control time, or launch range, ϵ_{r_T} in linear measure remained essentially constant; decreased range to target compensated for increased angular ϵ_{r_T} . Thus, there seemed to be a firing range (here, about 12,000 feet) below which no significant increase in accuracy was achieved.

Pilot proficiency and learning. - It can be seen from table VI that there was little variation in ϵ_{r_T} scores among the individual test pilots; even the relatively high CPE scored by pilot E for the 8,000-foot runs is probably nondefinitive. It should be noted, however, that the pilots who participated in this program were test pilots with engineering backgrounds and with previous experience in comparable optical simulators and tracking tasks.

Early in the test program, before the recording of miss data was begun, pilots A, B, and C made several simulator check-out and adjustment flights, during which their control techniques were developed at least to some extent. Pilots D and E had had experience in other Bullpup simulators before making the flights reported here. Obviously, learning curves constructed from the miss data, for any of the test pilots, would be of questionable value. However, some interesting qualitative observations are possible. The number of firings by pilots A, B, and C to attain the proficiency indicated in table VI was moderate (about 20 or 25). Pilot D, who had previous experience in the operation of a ground Bullpup simulator, made the transition to the Ames airborne equipment with little difficulty, attaining the indicated proficiency after 5 or 6 firings against the test target. Pilot E, who had had considerable flight experience with another airborne Bullpup simulator, made the transition easily, though the performance characteristics of the two simulators were quite different. Of course, the facility with which the transition is made from ground simulator to airborne simulator, or to the actual missile, may be affected by the handling qualities of the launch airplane (e.g., large or erratic trim changes during an attack).

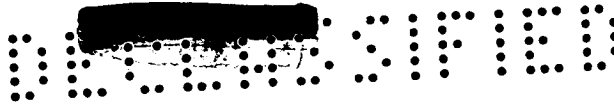
There was no appreciable loss in pilot proficiency after a layoff of as long as one month - at least for pilots A and B, the only pilots whose participation in the tests was not continuous from day to day.

Simulated Attacks on Typical Military Targets

On the basis of several impromptu attacks against readily visible ground targets: moving trains, trucks, and ships, the pilots formed the opinion that such targets were no more difficult to track with the simulator, using normal test attack techniques, than was the stationary test target.

Data from the film records of attacks against ground targets were insufficient for detailed statistical analysis. However, a brief examination indicated miss errors of the same order as against the test target.

Several simulated attacks against relatively slow, propeller-driven aircraft were made at low altitude (less than 10,000 feet) and under good visibility conditions. It was the pilots' opinion, at least for these conditions, that attacks with missiles employing Bullpup type guidance systems would require no unusual control procedures and that reasonable probable miss distance could be expected.



CONCLUSIONS

An airborne missile simulator was used to represent visually the predicted flight behavior of the Navy XASM-N-7 Bullpup air-to-surface missile, which is guided along the line of sight to the target by bang-bang radio signals controlled by the pilot of the launching airplane. The accuracy with which this missile (insofar as represented by the simulator) can be guided was assessed in simulated attack runs against a ground test target. Runs were made for firing ranges of 15,000 feet and 8,000 feet, with and without initial missile dispersion, at nominal attacker indicated airspeed of 350 knots and a dive angle of 20° . Five pilots with varying degrees of experience in this control task participated in the tests.

The results led to the following conclusions:

1. Quantitative response measurements showed that the airborne missile simulator gave a good representation of the trajectory and control characteristics predicted for the Bullpup missile, and the simulation appeared plausible to the pilots.

2. With no initial dispersion, the miss angle (the angle at impact between the line of sight to the target and the line of sight to the missile) for 50 percent of the firings was less than 3.5 milliradians (circular probable error in angular measure) for the 15,000-foot firing range and less than 4.2 milliradians for the 8,000-foot firing range. The greater circular probable error for the short-range firings was attributed to the decreased time available to the pilot for missile control. However, due to the shorter impact range for the 8,000-foot firings, the linear circular probable error measured normal to the line of sight to the target was less (20 feet) than for the 15,000-foot firings (29 feet).

3. With initial missile dispersion, no significant increase in circular probable error was observed, though the pilots considered the missile control task more difficult.

4. There was no evidence of marked differences in missile guidance proficiency among the test pilots. The number of simulated firings required to attain reasonably constant proficiency was moderate (of the order of 25), particularly for pilots with previous experience on other simulators. There was no evidence of appreciable loss in proficiency after a pilot layoff of as long as one month.

5. Occasional impromptu attacks were made, using normal test attack techniques, against readily visible targets (moving trains, trucks, and

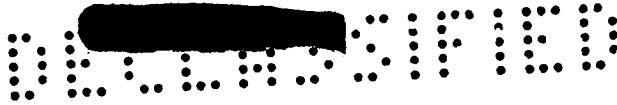


03710: [REDACTED] 30

ships). Pilots' opinions and motion pictures indicated that miss distances comparable to those against the test target could be expected.

Ames Aeronautical Laboratory
National Advisory Committee for Aeronautics
Moffett Field, Calif., July 24, 1956

[REDACTED]



APPENDIX A

MISSILE SIMULATOR COMPONENTS

Following is a description of the components of the airborne missile simulator sketched in figure 2. A description of ground tests of simulator performance is included.

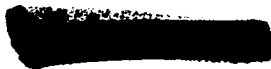
Missile Analog Computer

The rate of rotation of LS_M with respect to a fixed-space axis (fig. 21) is given by the equation:

$$\dot{\angle} LS_M = \frac{v_{OM} - v_{OA} + \int (A_M \sin \phi + a_M \cos \phi - A_A \sin \psi - a_A \cos \psi) dt}{\int \left[\cos \phi \left(v_{OM} + \int A_M dt \right) - \cos \psi \left(v_{OA} + \int A_A dt \right) \right] dt}$$

Since the error angle, ϵ_{LS} , between LS_T and LS_M is always small (almost never more than 10 milliradians), the angle ϕ between LS_M and the missile flight path is always small; and since immediately before firing, and throughout the run, the pilot maintains the airplane flight path essentially along LS_T , the angle ψ is small (nearly equal to ϵ_{LS}), and a_A and v_{OA} are essentially zero. Also, A_A is very nearly zero since the airplane is flown at nearly constant speed, V_A . The following approximations are therefore valid:

$A_A \approx 0$	$v_{OA} \approx 0$
$a_A \approx 0$	$\sin \phi \approx 0$
$v_{OA} \approx V_A$	$\cos \phi \approx 1$
$v_{OM} \approx V_A$	$\sin \psi \approx 0$
$\int A_M dt \approx V_M - v_{OM} = V_M - V_A$	$\cos \psi \approx 1$



Line-of-sight rate then can be approximated well within 5 percent:

$$\dot{\angle}LS_M = \frac{v_{OM} + \int a_M dt}{\int (V_M - V_A) dt}$$

Since V_A is maintained at a preselected value during a test run,

$\int (V_M - V_A) dt$ may be replaced by a programmed value of the range R .

This approximation of $\dot{\angle}LS_M$ contributes to a more simple simulator since it requires fewer quantities to be measured and to be considered in the missile analog computer.

Of course, random airplane accelerations (e.g., due to rough air) introduce errors into the approximations $a_A \approx 0$ and $\psi \approx 0$; however, these errors have no significant effect upon the validity of the simplified expression for $\dot{\angle}LS_M$. It is estimated that their maximum effect, 1 second after firing, would be about 7 milliradians; 2 seconds after firing, about 2 milliradians; 4 seconds, about 1/2 milliradian (imperceptible).

Let us consider now a conventional computer (fig. 22) which might be used to simulate the behavior of LS_M . The pilot's command signal is sent to a missile control-servo analog computer. Output of the servo computer is fed to a missile aerodynamics analog computer, coefficients of which are programmed functions of missile Mach number (or time after launch). A voltage representing the acceleration due to gravity, for the elevation channel, or due to cross wind, for the azimuth channel, is added. The resultant voltage, an analog of missile acceleration normal to LS_M , is integrated, and to the result the initial dispersion velocity signal is added. The sum is divided by the programmed value of range from airplane to missile and the quotient applied to the space reference system as a line-of-sight rate of rotation signal.

The airborne missile analog computer used in the present test program resembles closely the conventional computer just discussed, but for one simplification. The control servo and missile aerodynamics transfer functions were combined into one first-order approximation, $K/(1 + \tau_e p)$. The quantity τ_e is the time constant which gives the best first-order approximation of the combined servo and missile response. Presented in figure 23, for the conventional and the approximate analogs, are computed time histories of the acceleration, velocity, and displacement responses to a step η command of 7.3g, the maximum available (fig. 3). In addition, the difference between the two displacement curves (the error in displacement) is plotted to a large scale. It can be seen that the error introduced into the transient acceleration response is sizable; however,



the error in displacement is less than 1 foot. The maximum displacement error in angular measure (the primary quantity observed by the pilot) would result from a step command applied immediately after firing and would be about 1 milliradian. For a step command applied 3 seconds after firing, maximum error would be about 0.5 milliradian; 10.8 seconds after firing, about 0.06 milliradian. Since these values of error are, in general, less than a pilot's threshold of visual perception, the first-order representation of control servo and missile aerodynamic response and the attendant simplification of electronic circuitry are considered satisfactory for the present program.

Figure 24 is a simple block diagram of the elevation channel of the airborne missile analog computer used for these tests. It can be seen by comparison with figure 22 that the present simulator is essentially a conventional simulator incorporating the response approximation just discussed. In addition to the elevation channel (fig. 24), there is a similar azimuth channel in which the gravity signal is omitted. The programmer provides a voltage proportional to the available missile load factor, η , which is picked off a potentiometer whose slider follows a cam contour cut according to the variation of η with time after launch (fig. 3). Another cam positions the slider of the range potentiometer in accordance with the change in range from launch airplane to missile (fig. 3). A constant-speed electric motor drives both cams.

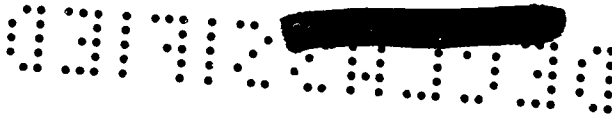
The pilot's command switch is an eight-position spring-return toggle switch, through which he can apply the η voltage available at the programmer to the missile response computer as an up, down, left, or right command or as a 45° combination of an azimuth and an elevation command.

The missile response computer is a simple resistance-capacitance (R-C) network whose output is an analog of missile response to η . A constant voltage representing $1g$ gravity acceleration is added to the output of the response computer, and the resultant missile acceleration signal, a_M (normal to LS_M), is applied to the integrator, an R-C network.

Output of the integrator represents the change in missile velocity, Δv_M , normal to LS_M . Added to Δv_M , when desired, is a voltage representing a velocity bias, v_{OM} , due to missile dispersion at launch (initial missile dispersion). The resultant missile velocity voltage, v_M , is divided, in a high gain feedback amplifier, by the range, R , from the programmer. Output of the amplifier, the final output of the missile analog computer, is the signal representing v_M/R , or line-of-sight rate of rotation in space, $\angle LS_M$.

The time histories of η and of R for which the programmer cams were cut were obtained from the XASM-N-7 contractor and are shown in figure 3.



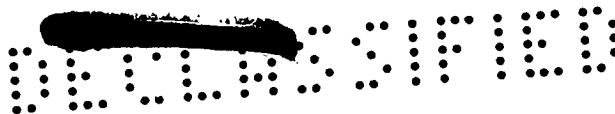


Gyro Stabilized Reference and Optical Presentation

The space stabilized reference system and the optical presentation device shown in figure 2 are diagrammed in more detail in figure 25. The stabilization loop is a modified radar antenna drive circuit from an E-3 fire-control system; the optical presentation device is a modified A-4 optical gunsight head. The sight head mirror drive system is essentially slaved to the antenna axis. Precession of the antenna axis according to $\angle LS_M$ produces corresponding precession of the sight head mirror position, and the resultant motions of the collimated dot on the airplane windshield represent to the pilot the change in orientation of LS_M .

Since they were unnecessary for the present tests the antenna dish and dipole, as well as the roll resolution loop used in the target simulator program (ref. 1), were removed. The term antenna as used hereafter shall imply only the HIGU stabilization gyros and the gimbals of the original E-3 radar antenna. The gimbals allow the antenna two degrees of freedom about axes parallel to the airplane yaw axis (antenna azimuth axis) and normal to the yaw axis (antenna elevation axis). Two single-degree-of-freedom type HIGU integrating gyro units (with integral torque and signal generators) are rigidly fixed to the antenna, their axes of precession respectively parallel and normal to the antenna elevation axis. The HIGU integrates the difference between the true rate of rotation of the antenna, sensed mechanically, and the desired rate of rotation, represented by an external electrical signal applied to the torque generator. When the external electrical signal is zero, any disturbance tending to cause rotation of the antenna is sensed by the HIGU. Output of the HIGU signal generator is fed to an electric motor which drives the antenna at the correct angular velocity with respect to the airplane to cause zero antenna rotation in space. Thus, the antenna provides a stabilized reference axis. When an electrical signal is applied to the HIGU, the output signal causes the drive motor to rotate the antenna at an angular velocity in space proportional to the value of the input signal. The integrating feature of the HIGU assures that the antenna will rotate through an angle equal to the time integral of the desired rate, regardless of dynamic lags in the system. An antenna position pickoff measures continuously the angle between the antenna axis and the airplane reference line, $\angle AL-RL$.

The antenna pickoff output is sent to the mirror drive loop summing point (fig. 25) in the A-4 gunsight head, to be added to the signal from the mirror position pickoff, $\angle RL-ML$, the angle between mirror axis and airplane reference line. In the antenna and mirror drive loops of the E-3 fire-control system and the target simulator, $\angle AL-RL$ and $\angle RL-ML$ were the only inputs to the summing point; output was the error signal $\angle AL-ML$. Servo action of the loop kept $\angle AL-ML$ essentially zero, hence, the mirror axis was continuously aligned with the antenna axis. The apparent position of the collimated dot projected onto the airplane windshield varied as the orientation in space of ML and, hence, of AL .



Initially it was intended that the antenna-mirror-drive circuit for the missile simulator be adapted "as is" from the target simulator; but unsatisfactory response to typical step acceleration signals was recorded during early ground tests. Results of the tests for representative step η/R commands are presented in figure 26. Time histories of the square root of displacement are plotted so that the slope is a measure of the square root of angular acceleration. Actual response of the antenna-mirror-drive system was measured at the sight head mirror since simulated missile motion is exactly twice mirror motion. Note the large initial time lags in the response of the original loop. (Note, however, that the integrating property of the HIGU tended to wipe out the large initial errors in displacement.) Response measurements at the antenna showed the mirror position was accurately following antenna position. Thus, it seemed that the dynamic response of the antenna itself was not adequate for this unusual application.

To obtain improved simulator behavior through improved antenna response would entail extensive modification of the antenna drive circuit. A more direct approach, to drive the mirror according to the desired LS_M signal, appeared to be also simpler to effect. Accordingly, the original circuit was modified (fig. 25) so that the antenna error signal available at the output of the HIGU is applied as a correction signal at the mirror drive loop summing point; it follows that resultant mirror drive signal is

$$\underline{\sqrt{LS_M-ML}} = \underline{\sqrt{LS_M-AL}} + \underline{\sqrt{AL-RL}} + \underline{\sqrt{RL-ML}}$$

and mirror position is nulled continuously with desired LS_M . Results of ground tests of the modified circuit (fig. 26) showed excellent dynamic response at the sight head mirror.

A block diagram of one channel of the Ames airborne missile simulator, used in the present test program, is presented in figure 27.





APPENDIX B

IN-FLIGHT PERFORMANCE CHECKS

Figure 28 is typical of the response curves obtained from the antenna-mirror stabilization performance check made during each test flight. With the stabilization check switch (fig. 8) open, so only the space-stabilization signal from the HIGU would affect $\angle AL$ and $\angle ML$ (fig. 25), the pilot flew the airplane toward some far distant object (a mountain peak, a cloud formation), fired the simulator, and then oscillated the airplane in pitch and in yaw while motions of the airplane and the missile dot relative to the distant object were recorded by the sight head camera. A measure of airplane pitch and yaw oscillations was obtained from the apparent motion of the object in successive data film frames. Changes in position of the missile dot relative to the object, as the airplane oscillated, were also read from the film.

The curves of figure 28, typical of the data from the space-stabilization check run made during each flight, show that the stabilization system rejected 95 percent of the amplitude of disturbing oscillations at the airplane natural frequency in pitch and in yaw. On none of the firing runs was the test pilot aware of any coupling between airplane and missile dot. The pilots commented particularly on the contrast in rough air between the difficulty of tracking the target with the locked reticle (as before firing) and the relative ease of tracking with the space-stabilized reticle (after firing).

Higher frequency oscillations (4 or 5 cycles per second) of a fraction of a milliradian amplitude were present in the reticle display but were noticeable by the pilot only on the space-stabilization check runs, and then only when the test airplane was in steady straight flight. This high-frequency "jitter" was of no consequence during a firing run.

The simulator was adjusted to keep azimuth and elevation drift to a minimum. In many of the runs in which the pilot fired the missile with zero initial azimuth error, no azimuth correction was required. Gravity drop simulation completely masked any elevation drift. In fact, several of the pilots suggested that because of the realistic gravity-drop simulation and low-drift characteristics, the simulator could be adapted for use as an airborne trainer for the firing of unguided rockets.





1. Doolin, Brian F., Smith, G. Allan, and Drinkwater, Fred J., III: An Airborne Target Simulator for Use in Optical-Sight Tracking Studies. NACA RM A55F20, 1955.
2. Anon.: Handbook Service Instructions, Type A-4 Gyro Computing Sight (Gun - Bomb - Rocket). Tech. Order No. 11F39-2-3-11, A C Spark Plug Co., 2 Nov. 1953.
3. Dixon, Wilfrid J., and Massey, Frank J., Jr.: Introduction to Statistical Analysis. McGraw-Hill Book Co., Inc., New York, 1951.
4. Burington, Richard S., and May, Donald C., Jr.: Handbook of Probability and Statistics with Tables. Handbook Pub., Inc., Sandusky, Ohio, 1953.



TABLE I.- MISS ANGLE IN MILLIRADIANS FROM 15,000-FOOT FIRING RANGE RUNS, NO INITIAL DISPERSION

x = azimuth miss

r = radial miss about center
of impact

y = elevation miss

r_T = radial miss about test target

Run	Flight no. 19 pilot A				Flight no. 20 pilot C				Flight no. 23 pilot C			
	x	y	r	r_T	x	y	r	r_T	x	y	r	r_T
1	2.6	2.6	2.6	3.7					-0.3	-2.9	5.1	2.9
2					0.3	6.0	3.9	6.0				
3												
4									.5	-1.6	3.8	1.7
5					-5.6	3.6	5.8	6.7				
6												
7					-.9	3.1	1.4	3.3				
8					-2.8	2.7	2.9	3.9	-.1	0	2.1	0
9					4.4	5.9	5.8	7.4				
10	-.9	-2.1	4.4	2.3	.6	3.9	1.9	3.9				
11	-.4	-.1	2.2	.4					.4	4.2	2.1	4.2

Run	Flight no. 24 pilot A				Flight no. 25 pilot B				Flight no. 26 pilot A			
	x	y	r	r_T	x	y	r	r_T	x	y	r	r_T
1	-0.5	2.7	0.7	2.8	-7.6	2.7	7.6	8.1	-3.3	4.1	3.8	5.2
2	3.3	2.2	3.3	3.9	-1.2	3.0	1.5	3.2	.1	3.8	1.7	3.8
3	0	2.6	.5	2.6	-.5	-3.3	5.5	3.4	7.5	-4.6	10.1	8.8
4	-.1	2.5	.4	2.5	.6	4.1	2.0	4.2	.9	1.9	1.2	2.1
5	.7	4.7	2.7	4.8	.8	2.8	1.1	2.9	.7	.8	1.5	1.1
6	-.6	2.5	.7	2.6								
7					1.3	1.3	1.6	1.9	3.6	1.9	3.6	4.0
8	-.3	4.2	2.1	4.2	2.3	2.5	2.3	3.4	.8	3.5	1.6	3.6
9	3.9	1.7	4.0	4.3	2.1	4.2	2.9	4.6	-1.1	2.1	1.1	2.4
10	-5.6	4.0	5.9	6.9	-2.2	-1.1	3.9	2.4	-.5	3.3	1.3	3.4
11	-2.0	1.9	1.9	2.8	-.9	6.1	4.1	6.2	4.0	5.5	5.2	6.8
12					-2.2	0	3.1	2.2	.9	3.5	1.8	3.7
13					-1.9	2.4	1.9	3.1	1.9	5.8	4.1	6.1

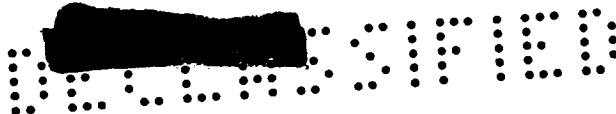


TABLE I.- MISS ANGLE IN MILLIRADIANS FROM 15,000-FOOT FIRING RANGE RUNS, NO INITIAL DISPERSION - Continued

Run	Flight no. 28 pilot B				Flight no. 29 pilot B				Flight no. 30 pilot A			
	x	y	r	r _T	x	y	r	r _T	x	y	r	r _T
1	-1.3	2.3	1.3	2.6	-0.4	1.0	1.2	1.1	2.4	0.2	3.1	2.4
2	-3.7	6.7	5.9	7.7	-3.8	3.8	4.1	5.4	.8	3.3	1.4	3.4
3	-2.0	4.4	6.9	4.9	-2.6	.6	3.1	2.7	.6	3.3	1.3	3.3
4	-5.8	1.0	5.9	5.9	.3	4.9	2.8	4.9	-3.8	2.2	3.8	4.4
5	1.3	1.3	1.5	1.8	-1.7	.2	2.6	1.7	.4	1.4	.9	1.4
6					1.7	2.4	1.7	2.9				
7	.6	1.4	.9	1.6					-1.6	4.8	.3	5.1
8	-.7	3.0	1.1	3.1	-5.7	1.4	5.7	5.8	-.2	3.0	.9	3.0
9	-2.2	1.6	2.3	2.7	-3.3	2.5	3.3	4.1	-2.3	4.0	2.9	4.6
10	-2.8	5.2	4.1	5.9	.4	-1.1	3.2	1.2	-1.1	1.9	1.1	2.2
11	-2.9	1.6	3.0	3.3	.3	1.4	.8	1.4	4.7	2.8	4.7	5.5
12	-1.6	4.7	3.0	5.0	-.3	-.7	2.8	.7	1.5	2.1	1.5	2.5
13	3.0	3.1	3.2	4.4	-2.1	1.4	2.2	2.5				

Run	Flight no. 42 pilot D				Flight no. 43 pilot E				Flight no. 44 pilot D			
	x	y	r	r _T	x	y	r	r _T	x	y	r	r _T
1					-4.5	5.7	5.7	7.3				
2	-1.6	0.2	2.5	1.6	2.6	1.5	2.7	2.9				
3	-3.5	.2	4.0	3.5	2.7	1.5	2.8	3.1				
4	6.7	.3	6.9	6.7	-4.0	.7	4.9	4.0				
5												
6					-2.0	4.7	3.3	5.1				
7					2.4	3.7	2.9	4.4	-3.4	1.3	3.5	3.6
8					-1.8	1.8	1.8	2.5	-2.8	2.2	2.8	3.6
9									5.9	-1.7	7.0	6.1
10									-.8	-.1	2.3	.8
11									-.8	-1.5	3.7	1.7



TABLE I.- MISS ANGLE IN MILLIRADIANS FROM 15,000-FOOT FIRING
RANGE RUNS, NO INITIAL DISPERSION - Concluded

Run	Flight no. 45 pilot E				Flight no. 46 pilot D				Flight no. 47 pilot D			
	x	y	r	r _T	x	y	r	r _T	x	y	r	r _T
1												
2	4.2	1.4	4.3	4.4	2.9	6.0	4.9	6.6				
3	6.1	-.4	6.7	6.2	1.1	-.8	3.1	1.3	3.0	1.6	3.0	3.4
4	-3.5	4.3	4.1	5.6	4.5	6.3	6.1	7.7	2.9	3.9	3.4	4.9
5	-1.1	2.5	1.2	2.7	3.0	.4	3.5	3.1	2.4	4.6	3.4	5.2
6	2.8	.4	3.3	2.9	-4.3	.3	4.7	4.4				
7	2.0	1.3	2.2	2.4	-2.9	3.3	3.2	4.4	1.4	3.9	2.3	4.2
8	-4.2	2.4	4.2	4.9	-1.4	4.7	2.9	4.9	2.0	5.6	4.0	5.9
9	.3	1.3	.9	1.4					-1.0	.2	2.2	.9
10												
11	.1	1.8	.3	1.9								
12	0	.7	.4	.7								

Run	Flight no. 48 pilot E			
	x	y	r	r _T
1				
2	2.3	1.6	2.4	2.8
3	-.4	1.2	1.0	1.3
4				
5				
6				
7				
8	1.3	1.9	1.3	2.4
9				
10	1.4	-2.0	4.3	2.4
11	-.1	3.5	1.3	3.4
12	10.8	3.7	10.9	11.4
13	2.4	1.7	2.4	2.9

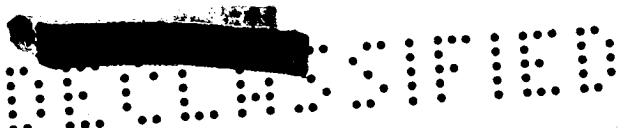


TABLE II.- MISS ANGLE IN MILLIRADIANS, FROM 15,000-FOOT FIRING RANGE RUNS, WITH INITIAL DISPERSION

x = azimuth miss

r = radial miss about center of impact

y = elevation miss

r_T = radial miss about test target

Run	Flight no. 55 pilot A				Flight no. 56 pilot B				Flight no. 57 pilot A			
	x	y	r	r_T	x	y	r	r_T	x	y	r	r_T
1					2.9	4.3	3.8	5.2	2.2	-10.2	11.4	10.4
2									.9	-2.2	3.3	2.3
3									5.9	-5.1	7.9	7.8
4	-1.2	2.9	3.2	1.2					-1.8	-2.6	4.6	3.2
5									.9	.7	.5	1.1
6												
7					1.8	4.6	3.6	4.9				
8	1.7	1.7	1.0	2.4					-.8	2.7	2.3	2.8
9	4.6	6.4	6.4	7.9	.9	1.3	.2	1.6	8.0	-3.7	8.6	8.8
10	-1.6	.4	2.5	1.6	4.7	4.2	4.9	6.4	0	1.1	.9	1.1
11	4.3	5.8	5.8	7.2	6.9	2.1	6.2	7.3	-.8	1.3	1.6	1.5
12	-1.7	4.1	7.9	4.4	-1.1	4.2	3.6	4.4	1.7	1.2	.8	2.0
13	.2	.9	.6	1.0	4.1	3.5	3.9	5.7	4.8	-2.4	5.3	5.4

Run	Flight no. 58 pilot A				Flight no. 59 pilot B			
	x	y	r	r_T	x	y	r	r_T
1	-1.4	3.6	3.3	3.9	1.8	2.3	1.5	2.9
2	-.2	4.7	3.7	4.7	-6.0	-2.8	7.9	6.7
3	-3.6	-2.5	5.8	4.4	-2.3	.1	3.4	2.3
4	-.7	1.9	1.7	2.2	1.3	-2.5	3.7	2.9
5	-1.2	3.3	2.9	3.8	-.4	-.7	2.2	.8
6								
7					-.5	2.4	1.8	2.4
8					-.3	.8	1.2	.8
9	3.6	2.6	3.1	4.4	-.8	-.6	2.5	.9
10	-.1	.7	1.1	.9	-1.8	-.2	2.9	1.8
11	1.7	-1.8	3.1	2.4	3.1	2.2	2.5	3.8
12	2.0	1.2	1.2	2.3	-1.9	2.4	3.1	3.1
13	3.6	1.8	2.8	4.0	.1	4.1	3.1	4.1



TABLE III.- MISS ANGLE IN MILLIRADIANS FROM 8,000-FOOT FIRING RANGE RUNS, NO INITIAL DISPERSION

x = azimuth miss

r = radial miss about center
of impact

y = elevation miss

r_T = radial miss about test target

Run	Flight no. 34 pilot A				Flight no. 35 pilot B			
	x	y	r	r_T	x	y	r	r_T
1	0.8	2.9	1.0	3.0	-0.3	1.3	1.3	1.4
2	1.6	2.8	1.3	3.2	5.9	5.2	6.5	7.8
3	-2.6	4.7	3.3	5.4	-1.3	2.0	1.3	2.4
4	-3.9	1.3	4.0	4.1	8.0	6.2	8.9	10.2
5	-3.4	5.7	4.5	6.7	4.7	7.6	6.9	8.9
6								
7	2.7	5.0	3.7	5.7	.4	2.7	.5	2.7
8	1.6	.4	2.7	1.6	-3.6	-.1	4.4	3.6
9	5.6	2.6	5.7	6.2				
10	.7	3.3	1.1	3.4				
11	-1.9	2.3	1.9	3.0	-1.8	1.5	2.1	2.4
12	-13.1	4.7	14.1	13.9				
13	1.8	2.2	1.9	2.9				
14	.2	.9	1.8	.9	8.1	.6	8.4	8.1
15	1.1	4.1	1.9	4.2				
16	-4.6	6.6	6.1	8.1				

Run	Flight no. 36 pilot B				Flight no. 37 pilot B			
	x	y	r	r_T	x	y	r	r_T
1	4.1	1.5	4.4	4.4	-1.8	1.7	1.9	2.4
2	6.4	-3.7	9.0	7.4	-.1	3.9	1.3	3.9
3	1.2	-.8	3.6	1.4	-3.7	1.6	3.7	4.0
4	2.8	3.2	2.9	4.3	-3.4	5.3	4.3	6.3
5	1.5	0	3.0	1.5	-2.5	-4.4	7.4	5.1
6								
7	1.9	5.8	3.8	6.1	-6.1	2.2	6.0	6.5
8	-.4	1.7	.9	1.7	4.7	1.0	5.0	4.8
9	2.8	.5	3.6	2.9	.2	4.4	1.8	4.4
10	2.3	3.0	2.5	3.8	-5.3	.4	5.7	5.3
11	-1.6	2.4	1.5	2.9	2.3	-.8	4.1	2.4
12	-.5	4.3	1.8	4.4	1.9	2.6	2.0	3.2
13	-2.8	.7	3.3	2.9	-7.2	2.4	7.3	7.8
14					-4.2	1.4	4.3	4.5
15					0	1.4	1.2	1.4



TABLE III.- MISS ANGLE IN MILLIRADIANS FROM 8,000-FOOT FIRING RANGE RUNS, NO INITIAL DISPERSION - Concluded

Run	Flight no. 38 pilot A				Flight no. 39 pilot A			
	x	y	r	r _T	x	y	r	r _T
1	-1.0	1.6	1.3	1.9	-3.1	4.2	3.3	5.1
2	-1.8	.9	2.4	2.1	-.2	1.6	1.9	2.4
3	-1.5	2.2	1.4	2.6	-3.2	2.6	3.1	4.1
4	-1.8	3.6	1.9	4.0	-6.8	3.7	6.8	7.7
5	-1.4	3.2	1.4	3.5	-.1	1.8	1.4	2.2
6								
7	7.7	5.4	7.7	9.4	-3.6	1.2	3.7	3.8
8	3.9	2.4	4.0	4.6	-1.1	3.2	1.1	3.3
9	0	0	2.6	0	1.6	2.8	1.7	3.2
10	-3.9	3.2	7.3	5.1	-6.2	3.2	6.1	6.9
11	-4.6	1.5	4.7	4.9	1.8	2.4	1.9	2.9
12	0	0	2.6	0	-1.8	0.1	2.9	1.8
13	1.2	0	2.9	1.2	3.8	4.2	4.2	5.7
14					-5.1	2.7	5.0	5.8

Run	Flight no. 49 pilot D				Flight no. 50 pilot E			
	x	y	r	r _T	x	y	r	r _T
1					0.8	6.4	3.9	6.4
2	2.2	3.8	2.5	4.3	-3.4	2.6	3.2	4.3
3	3.5	3.0	3.6	4.6	-2.3	2.0	2.3	3.1
4	3.5	2.2	3.6	4.1	-.9	5.0	2.6	5.1
5	3.6	.4	4.2	3.6	-4.8	1.8	4.8	5.1
6	2.7	5.4	4.0	6.1	-4.2	.8	4.5	4.3
7	5.4	3.9	5.7	6.6	-1.1	3.4	1.2	3.6
8					-.6	4.1	1.6	4.1
9	.6	.6	2.1	.8	1.7	-7.9	10.7	8.1
10					-5.0	6.0	5.9	7.8
11	2.2	4.0	2.7	4.6	-3.7	2.2	3.6	4.3
12					-.2	2.3	.3	2.3
13	3.2	.2	4.1	3.2	1.3	1.1	2.0	1.6
14					4.8	3.3	4.9	5.8
15					15.0	7.2	15.8	16.7
16					3.8	5.1	4.6	6.3
17					-3.9	4.1	4.0	5.6
18					-8.4	8.1	9.9	11.7



TABLE IV.- MISS ANGLE IN MILLIRADIANS FROM 8,000-FOOT FIRING RANGE RUNS, WITH INITIAL DISPERSION

x = azimuth miss

r = radial miss about center
of impact

y = elevation miss

r_T = radial miss about test target

Run	Flight no. 60 pilot A				Flight no. 61 pilot B			
	x	y	r	r_T	x	y	r	r_T
1	-0.7	2.5	2.4	2.6	-6.3	1.9	5.6	6.6
2	.6	10.0	1.6	10.0	-4.7	-1.0	4.8	4.8
3	3.5	-2.7	4.5	4.4	-4.0	5.7	5.3	7.0
4	7.3	5.1	9.7	8.9	5.4	-1.5	6.8	5.6
5	-2.1	1.3	4.0	2.4	1.2	5.2	3.9	5.3
6								
7	5.7	-6.7	7.5	8.8	.4	1.5	1.1	1.5
8	.2	-.3	1.0	.4	-2.9	-.6	3.2	3.0
9	-.3	-4.8	1.9	4.8	2.2	2.4	2.9	3.2
10	-1.9	-2.2	3.8	2.9	2.1	-4.0	6.3	4.5
11	4.4	2.7	5.7	5.2	-.2	4.9	3.3	4.9
12					-3.6	-2.8	5.3	4.6
13	2.2	2.4	3.4	3.2	1.0	4.2	3.1	4.3
14	-.4	6.2	2.1	6.2	-3.6	13.9	1.3	14.3
15					-5.5	.3	5.1	5.5

Run	Flight no. 62 pilot B				Flight no. 63 pilot A			
	x	y	r	r_T	x	y	r	r_T
1	4.9	11.4	3.7	12.5	-0.7	5.4	11.3	5.4
2	-4.0	-.8	.8	4.1	-.7	.8	4.1	1.1
3	2.5	1.0	7.2	2.7	-5.4	-3.8	3.2	6.6
4	.2	7.7	1.2	7.7	-.3	.5	6.1	.6
5	-5.4	-3.2	2.1	6.2	-2.4	.5	6.8	2.5
6								
7	-1.1	2.2	1.0	2.4	.1	.9	.7	.9
8	-2.4	.7	1.9	2.5	.6	3.2	2.0	3.2
9	-1.9	3.7	9.0	4.2	8.3	2.1	2.4	8.6
10	-3.5	1.7	4.9	3.9	-5.6	1.7	2.9	5.8
11	-.2	2.1	4.6	2.1	3.8	.5	.6	3.8
12	-2.2	4.8	2.3	5.3	-2.6	.3	3.6	2.6
13	.4	4.9	.6	5.0	-.9	1.1	3.5	1.5
14	-3.4	3.0	5.9	4.5	-6.3	-.1	3.0	6.3
15	-5.7	-1.0	9.7	5.7	8.5	4.9	5.7	9.8
16	2.2	2.9	5.9	3.6	-6.5	1.3	3.0	6.7
17	-3.2	1.3	4.3	3.5	3.4	0	2.6	3.4



TABLE V.- RECAPITULATION OF DATA FROM FIGURES 12 THROUGH 19

Launch conditions		No. of data runs	Mean point of impact, milliradians		Standard deviation, milliradians		Circular probable error			
			\bar{x}	\bar{y}	σ_x	σ_y	ϵ_r		ϵ_{r_T}	
							Milli-radians	Ft	Milli-radians	Ft
15,000-foot firing range 8,600-foot impact range 10.8-seconds missile flight time	No initial dispersion	127	0	2.1	2.7	2.1	2.8	24	3.4	29
	Initial dispersion	47	.8	1.2	2.9	2.7	3.2	27	3.3	28
8,000-foot firing range 4,700-foot impact range 5.5-seconds missile flight time	No initial dispersion	102	-.2	2.5	3.5	2.4	3.1	15	4.2	20
	Initial dispersion	58	-.6	1.6	3.9	3.4	3.6	17	4.5	21

TABLE VI.- CIRCULAR PROBABLE ERROR ABOUT THE TEST TARGET, ϵ_{r_T} , SCORED BY EACH PILOT, FOR THE VARIOUS TEST CONDITIONS

Pilots	15,000-foot firing range 8,600-foot impact range						8,000-foot firing range 4,700-foot impact range					
	No initial dispersion			Initial dispersion			No initial dispersion			Initial dispersion		
	No. of data runs	ϵ_{r_T}		No. of data runs	ϵ_{r_T}		No. of data runs	ϵ_{r_T}		No. of data runs	ϵ_{r_T}	
		Milli-radians	Ft		Milli-radians	Ft		Milli-radians	Ft		Milli-radians	Ft
A	36	3.4	29	28	3.3	28	40	3.9	18	28	4.1	19
B	36	3.4	29	19	3.3	28	35	3.9	18	30	4.5	21
C	10	3.6	31									
D	21	3.5	30				9	4.1	19			
E	24	3.5	30				18	5.3	25			

SECRET

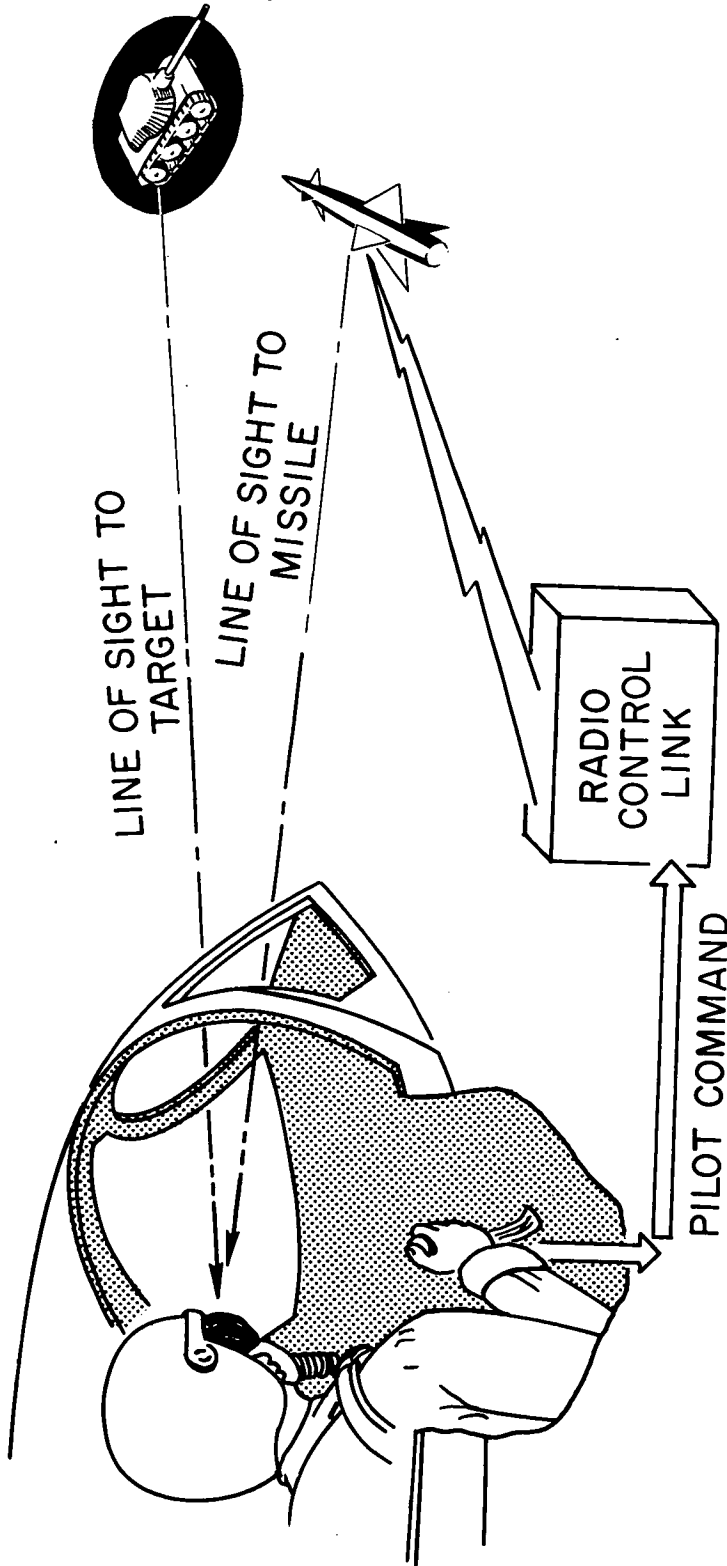


Figure 1.- Air-launched missile guided by pilot along visual line of sight to target.

SECRET

CONFIDENTIAL

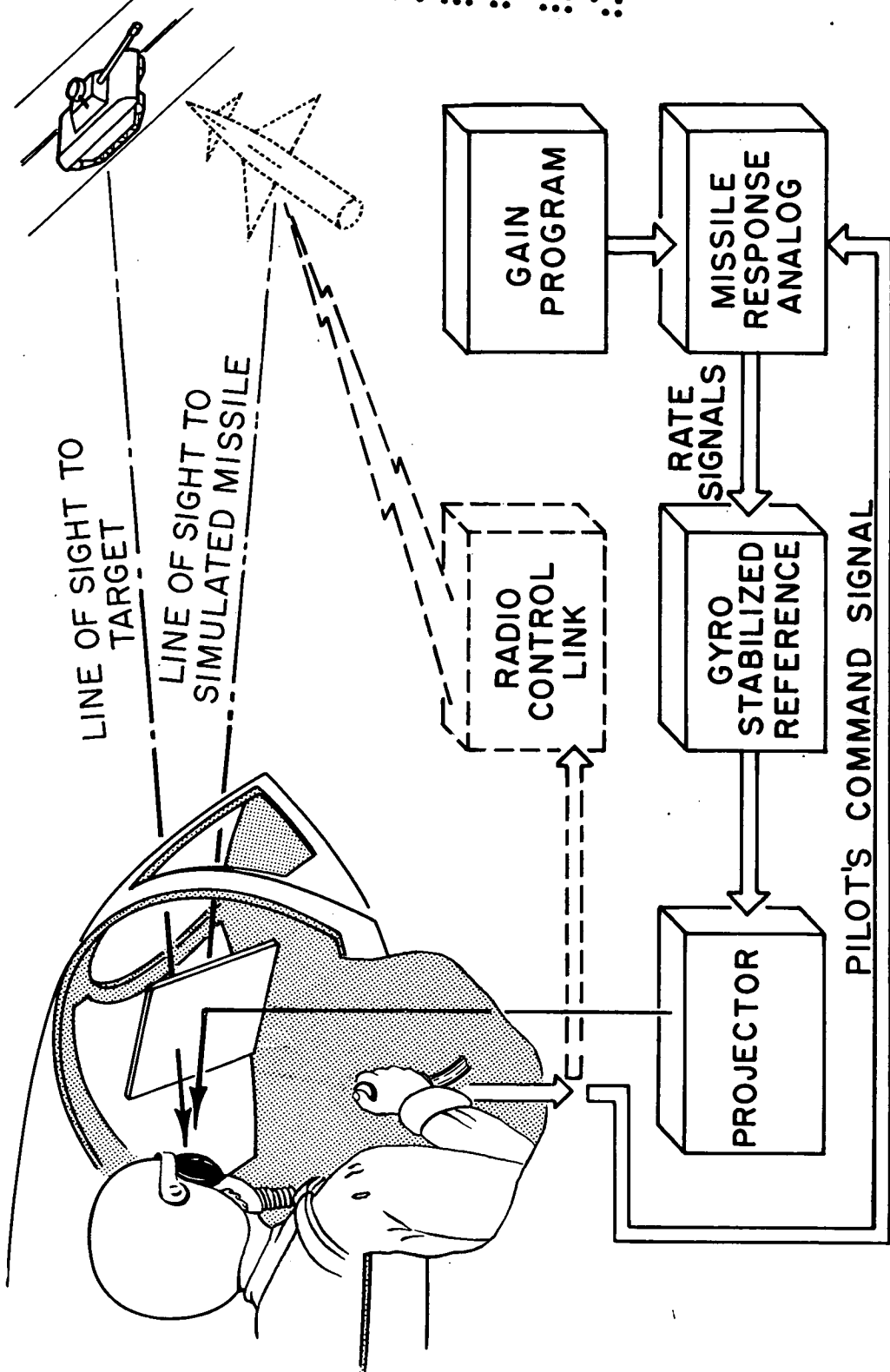


Figure 2.- Airborne missile simulator.

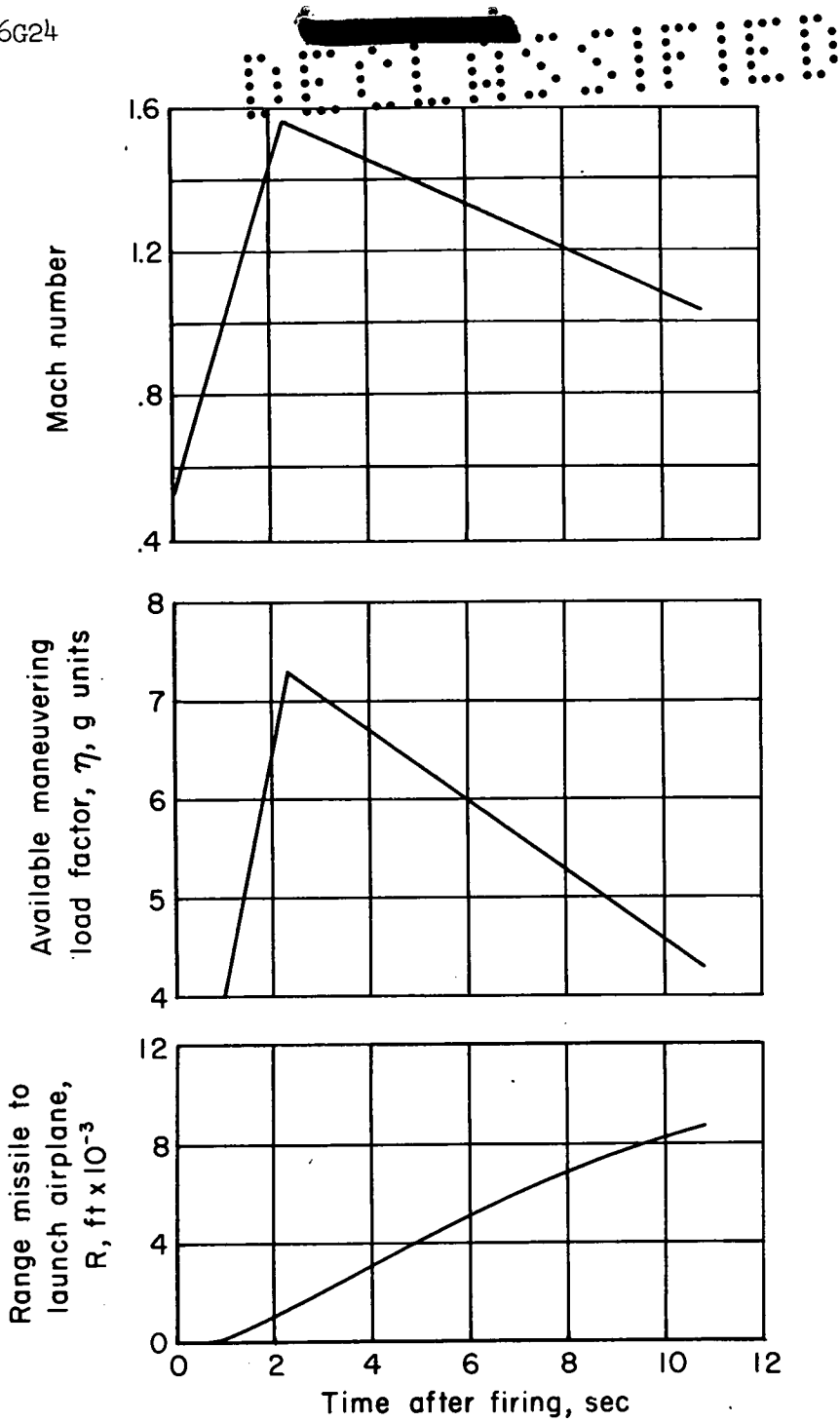


Figure 3.- Time histories of simulated missile characteristics.

~~CONFIDENTIAL~~



A-21015

Figure 4.- Test airplane.

~~CONFIDENTIAL~~

~~CONFIDENTIAL~~

CONFIDENTIAL

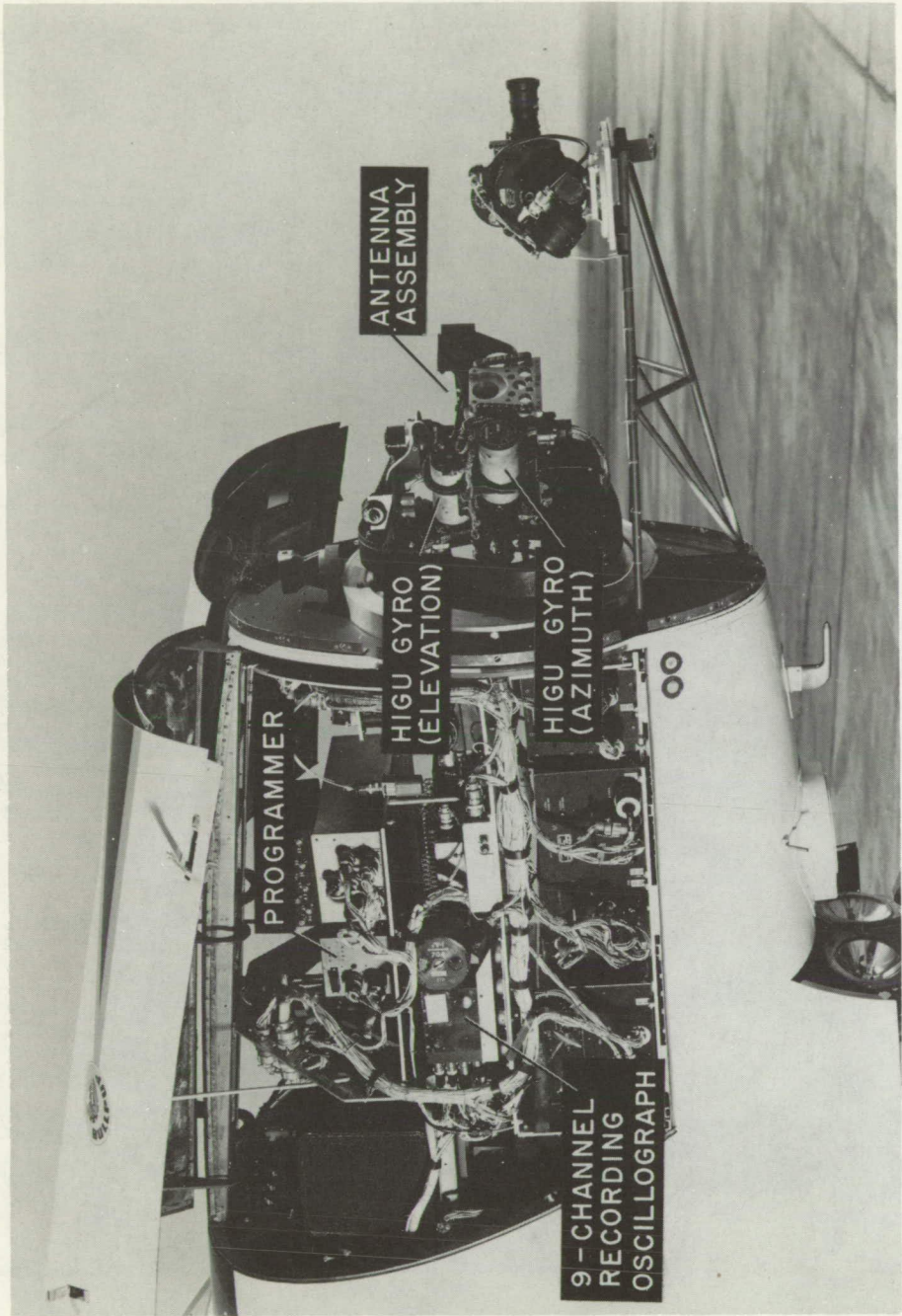


Figure 5.- Electronic components and antenna installation in test airplane.

~~CONFIDENTIAL~~

~~CONFIDENTIAL~~
03720000

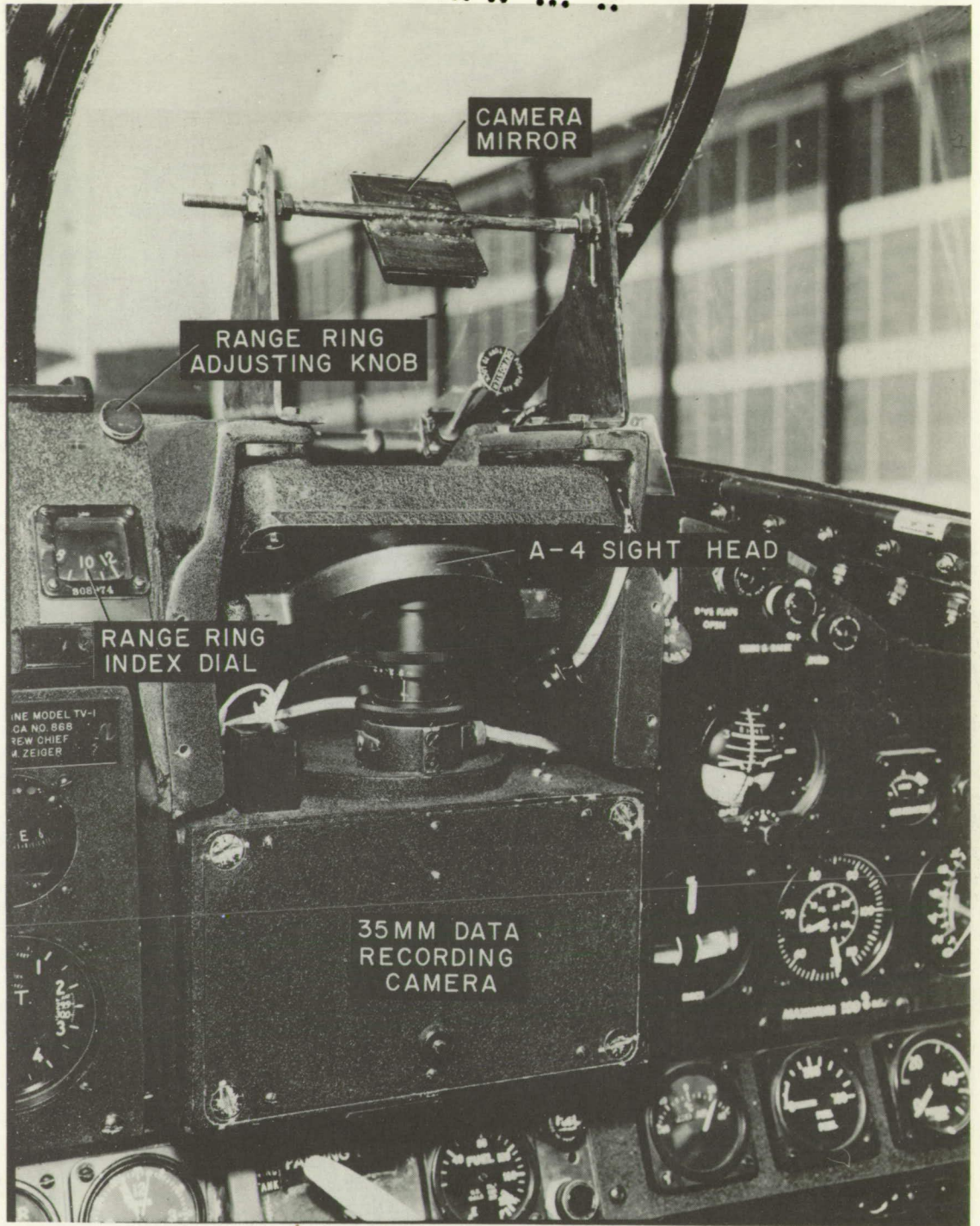


Figure 6.- Installation of A-4 sight head and photographic recording equipment.

CONFIDENTIAL

SECRET

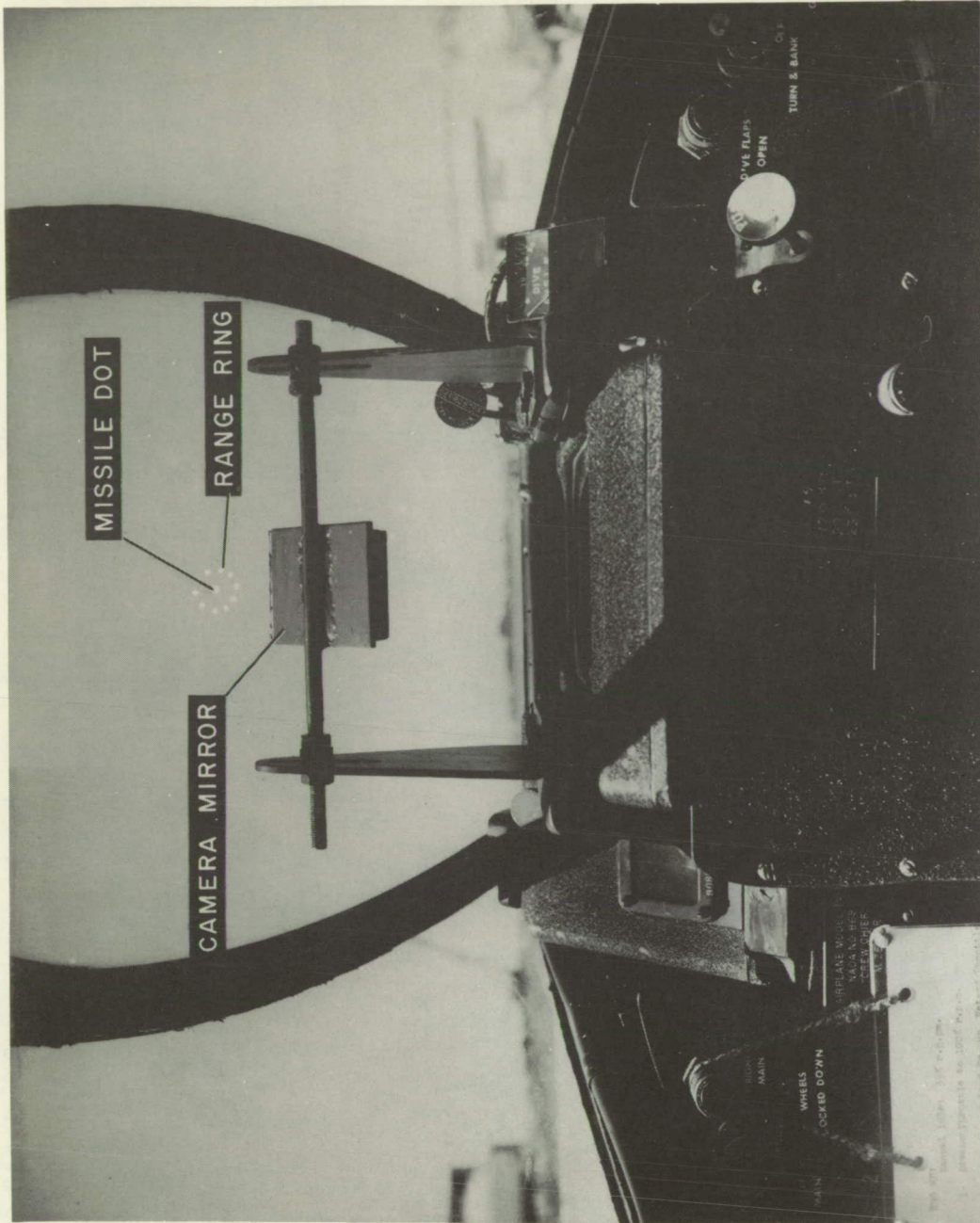


Figure 7.- Simulated missile dot and range ring as seen by pilot of test airplane.

CONFIDENTIAL

CONFIDENTIAL

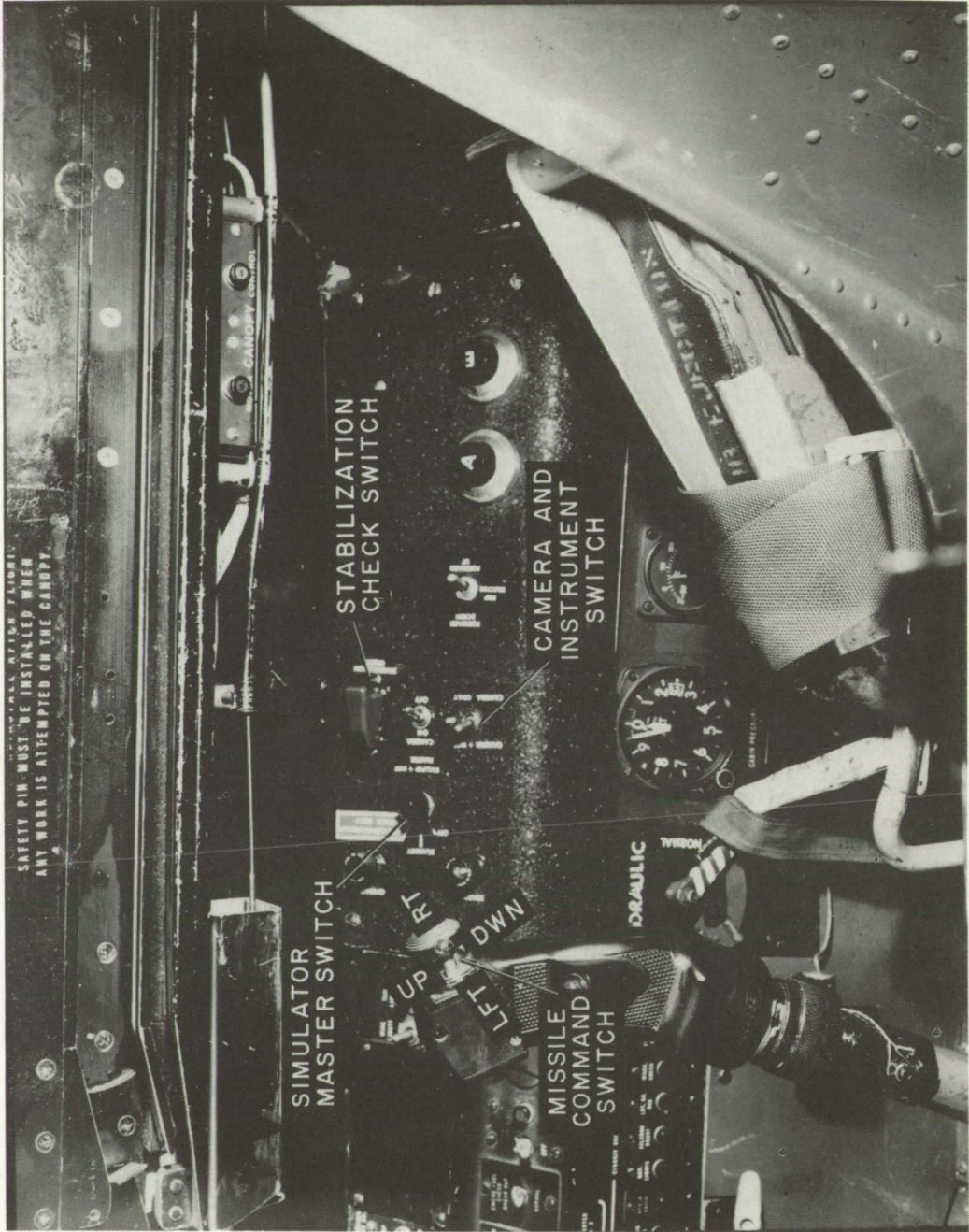


Figure 8.- Missile simulator command switch and switchgear panel in test airplane.

CONFIDENTIAL

~~CONFIDENTIAL~~ **CONFIDENTIAL**

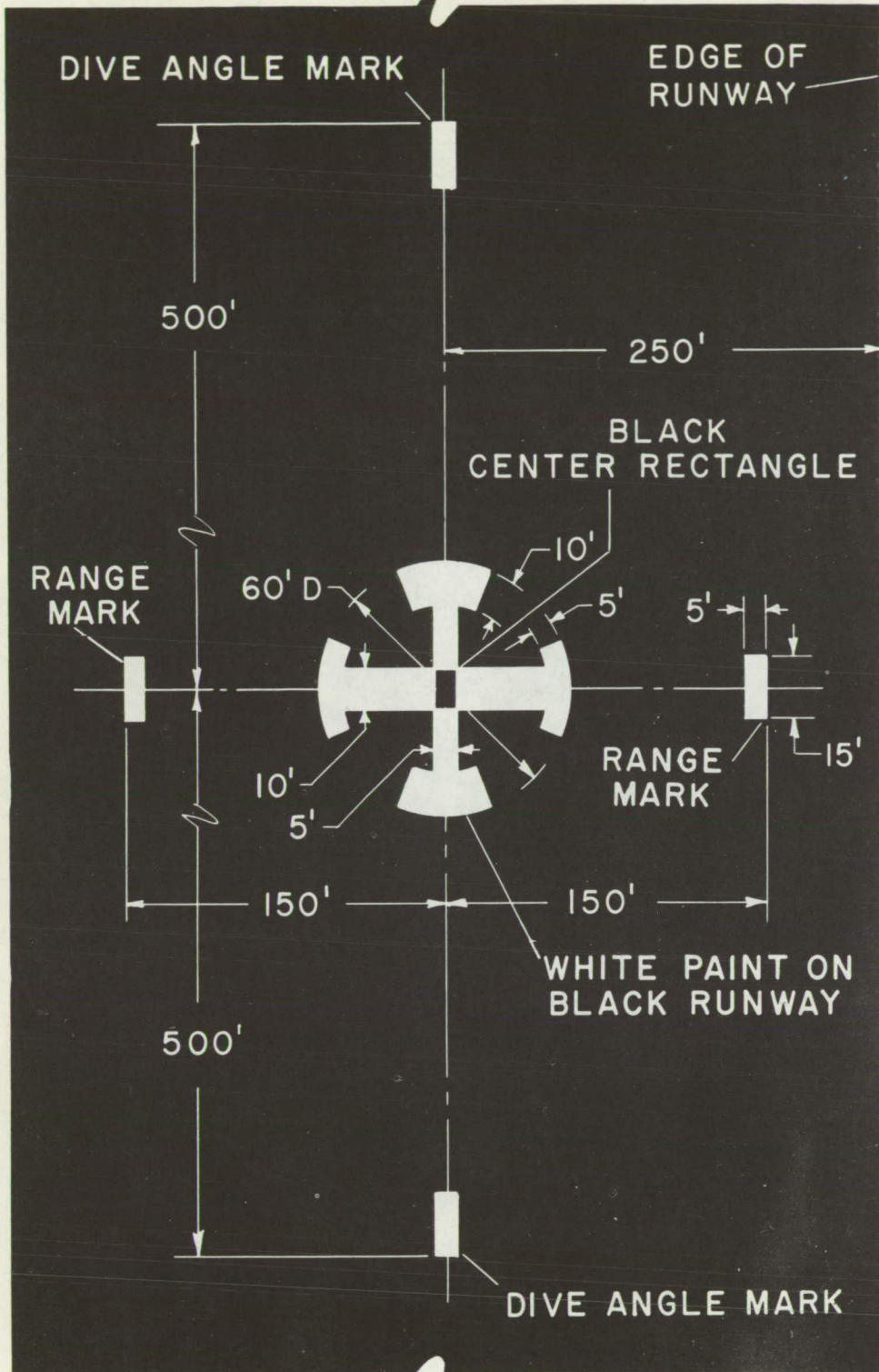


Figure 9.- Layout of test target.

~~CONFIDENTIAL~~ **CONFIDENTIAL**

~~CONFIDENTIAL~~

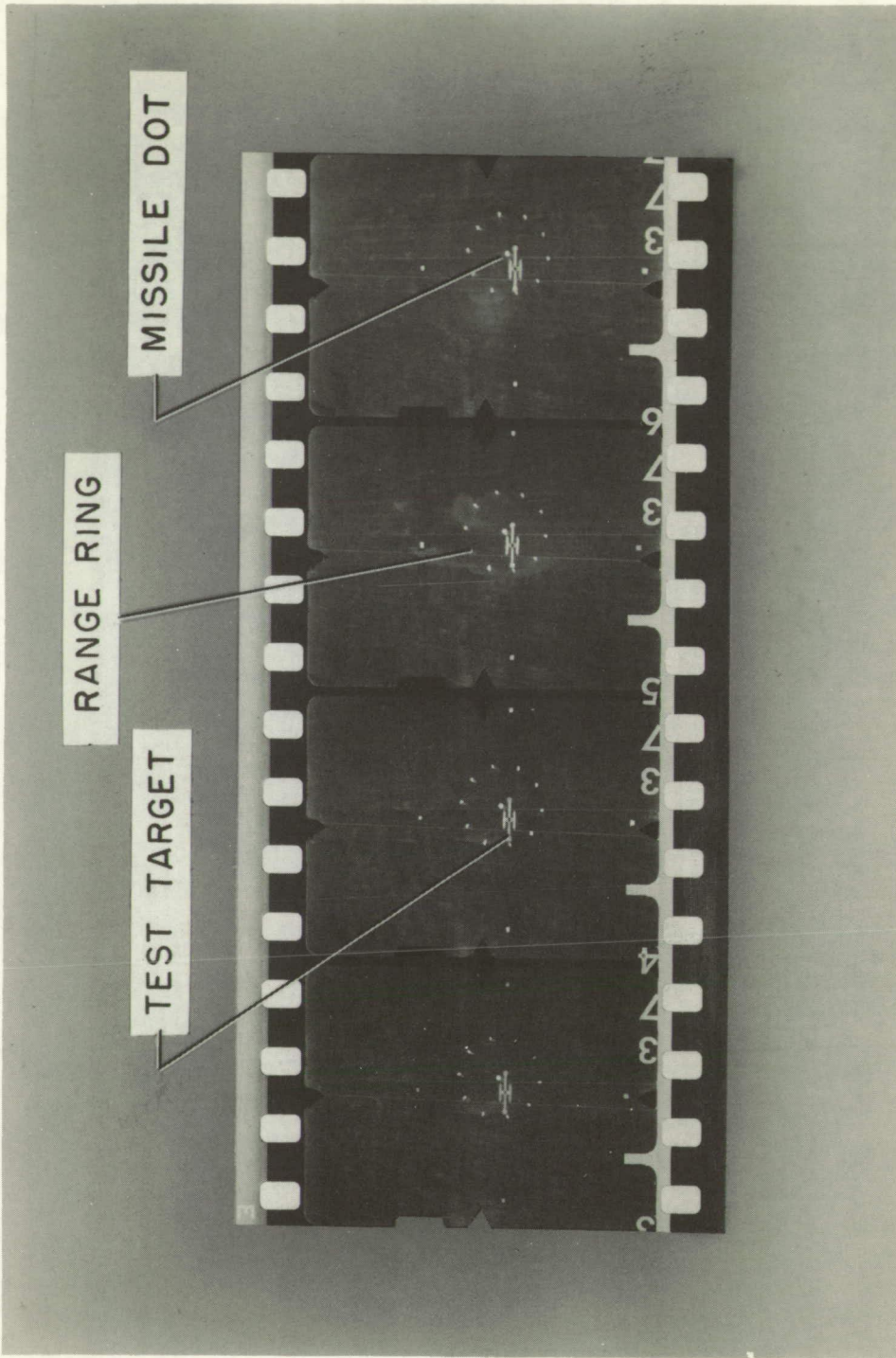


Figure 10.- Sample of 35mm data film.

~~CONFIDENTIAL~~

CONFIDENTIAL

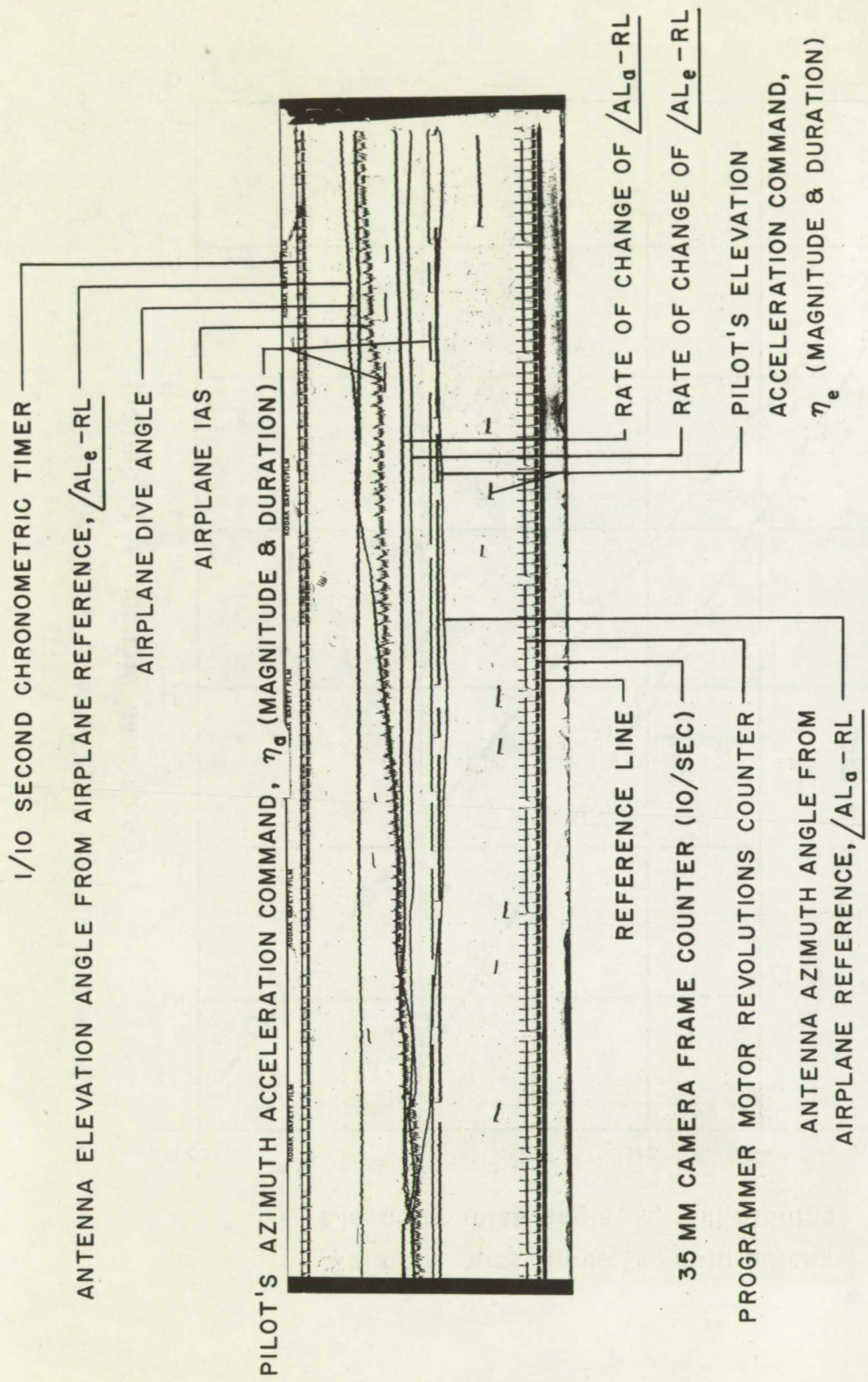


Figure 11.- Sample of nine-channel oscillograph color film record.

CONFIDENTIAL

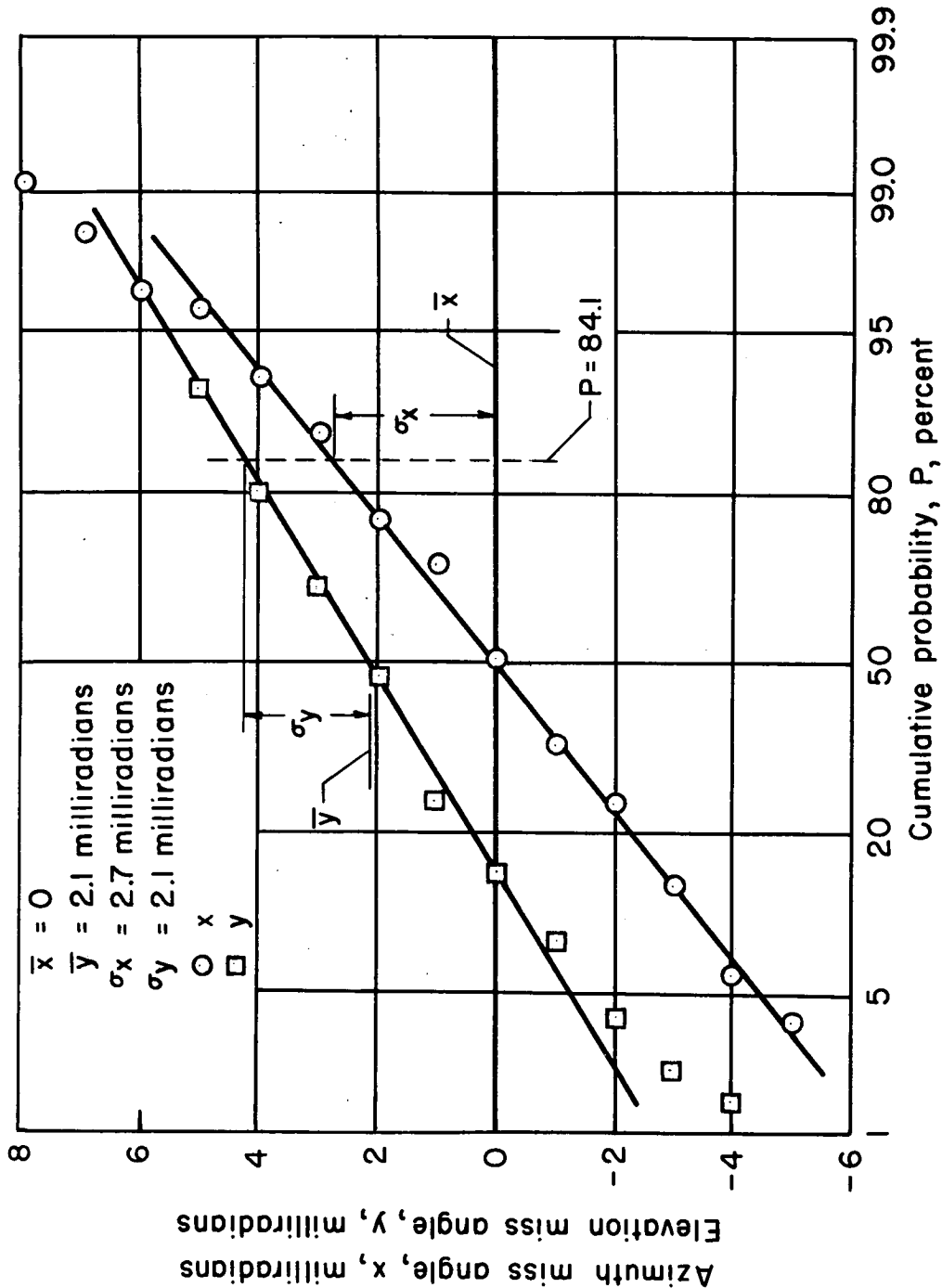


Figure 12.- Cumulative probability distribution of azimuth and elevation miss angles; 15,000-foot firing range, no initial dispersion.



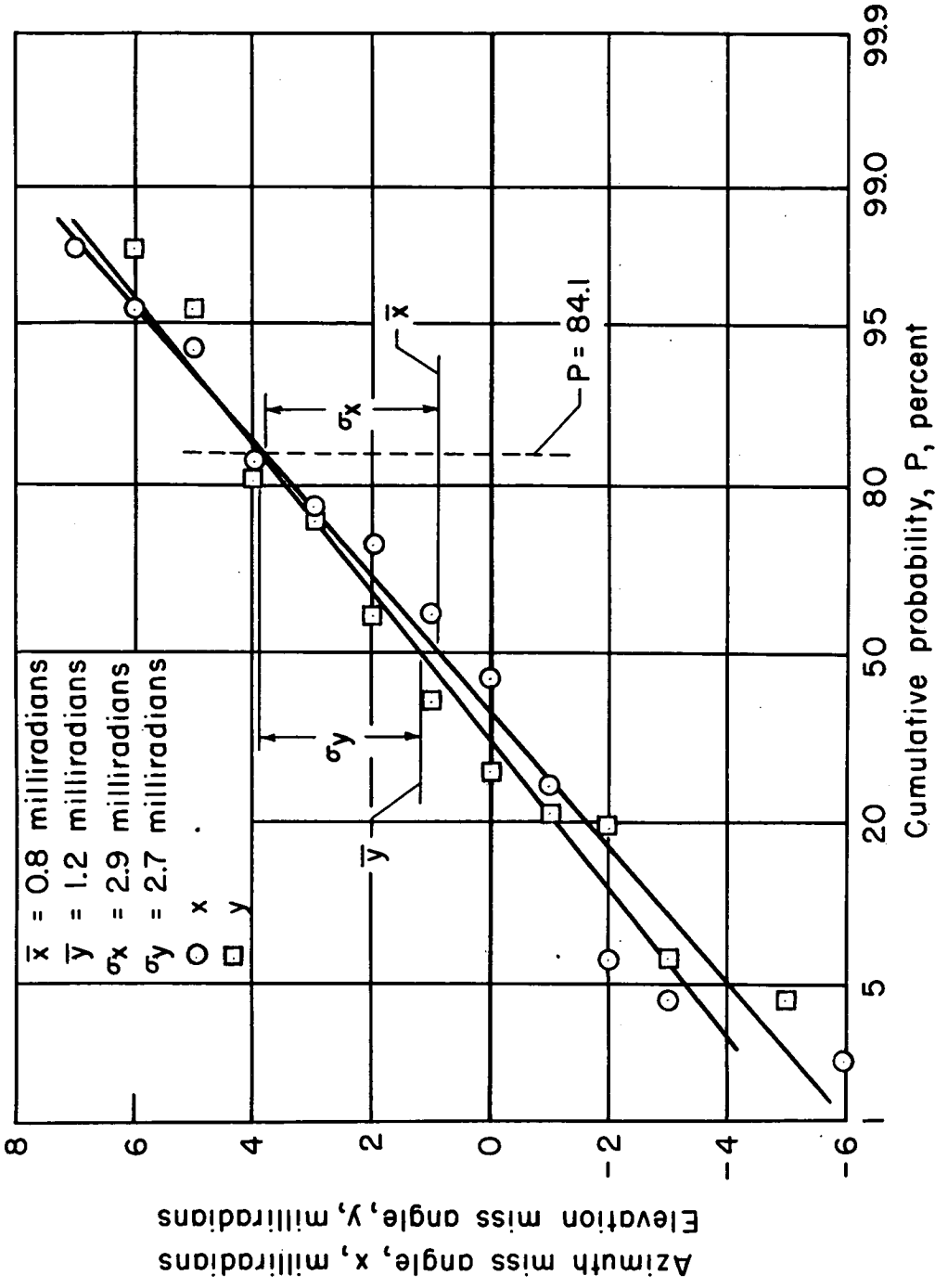
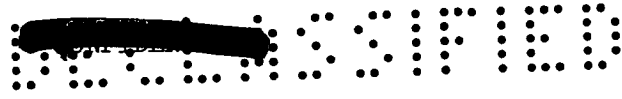


Figure 13.- Cumulative probability distribution of azimuth and elevation miss angles; 15,000-foot firing range, with initial dispersion.



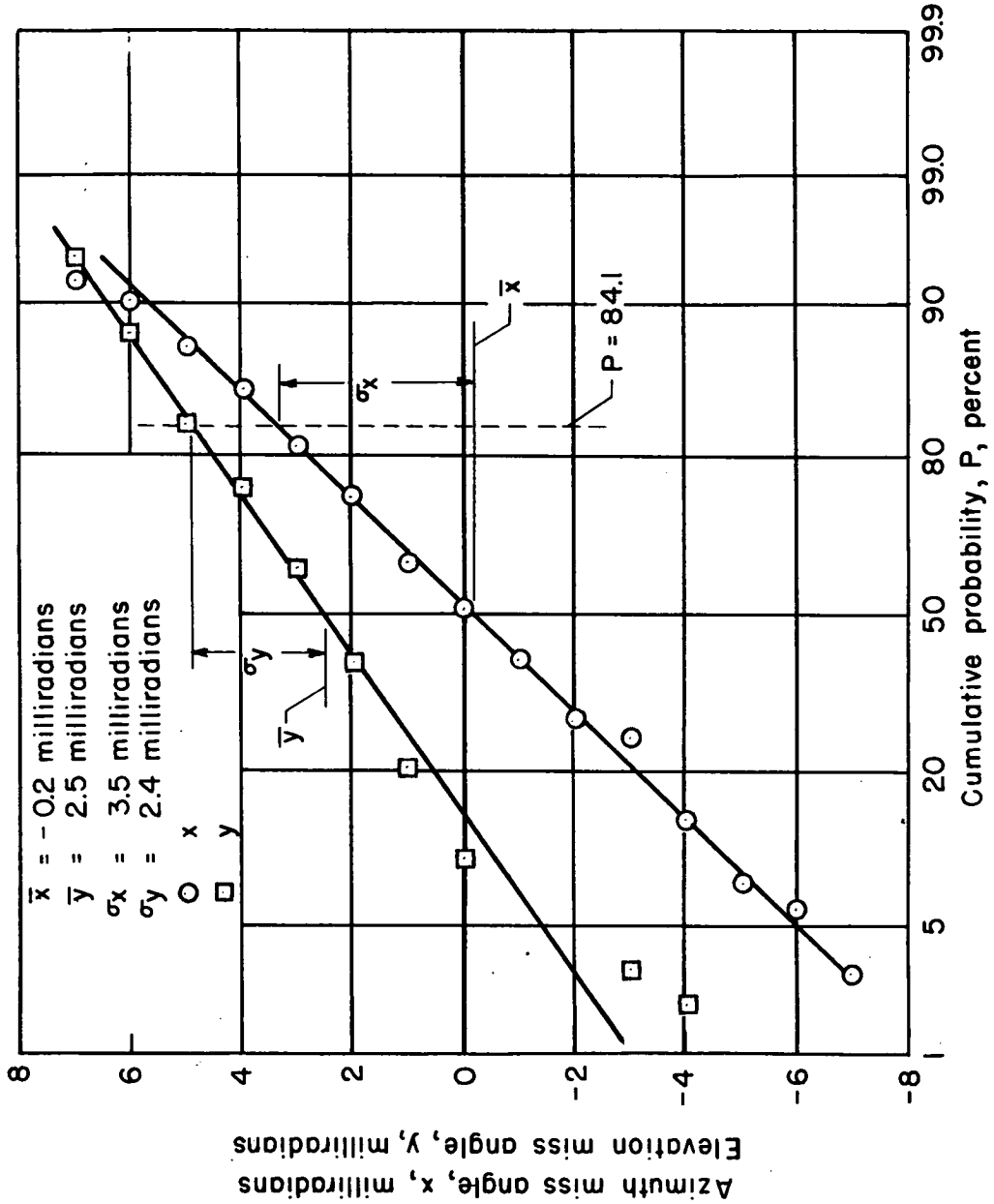
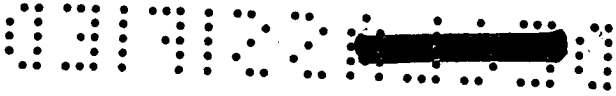


Figure 14.- Cumulative probability distribution of azimuth and elevation miss angles; 8,000-foot firing range, no initial dispersion.

CONFIDENTIAL

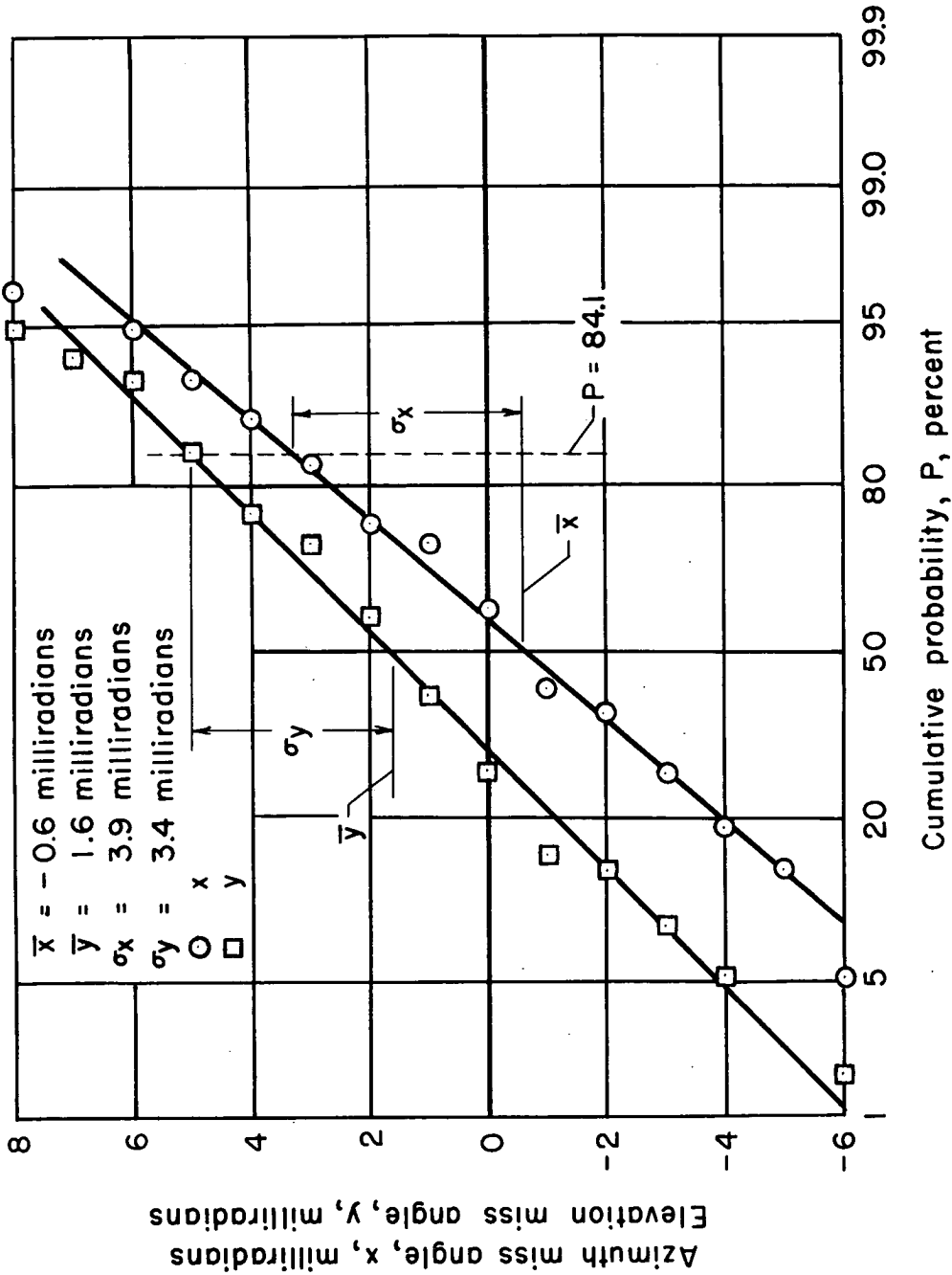


Figure 15.- Cumulative probability distribution of azimuth and elevation miss angles; 8,000-foot firing range, with initial dispersion.

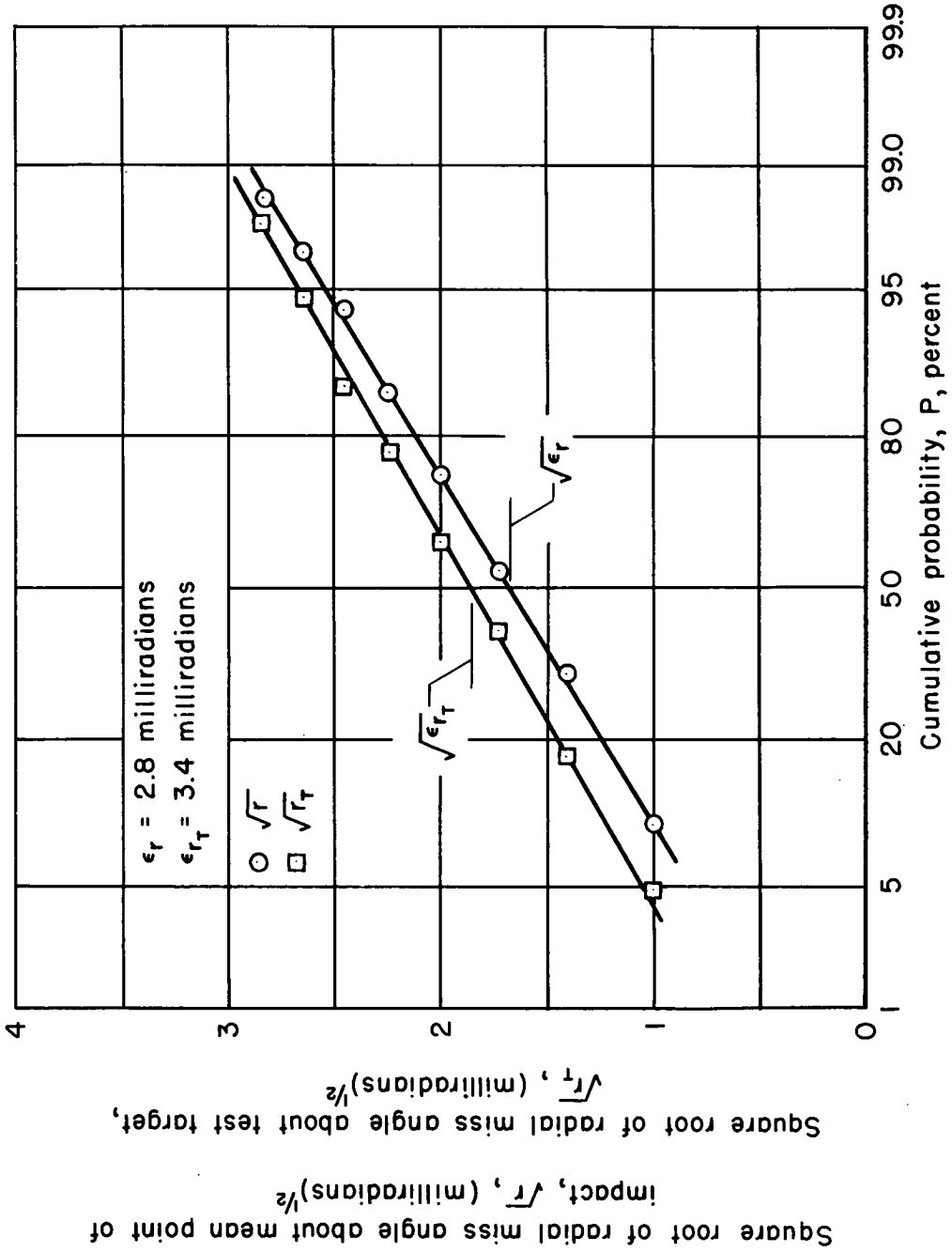
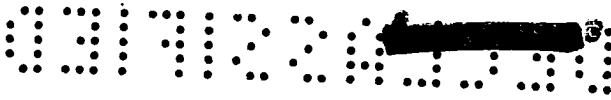


Figure 16.- Cumulative probability distribution of the radial miss angle; 15,000-foot firing range, no initial dispersion.

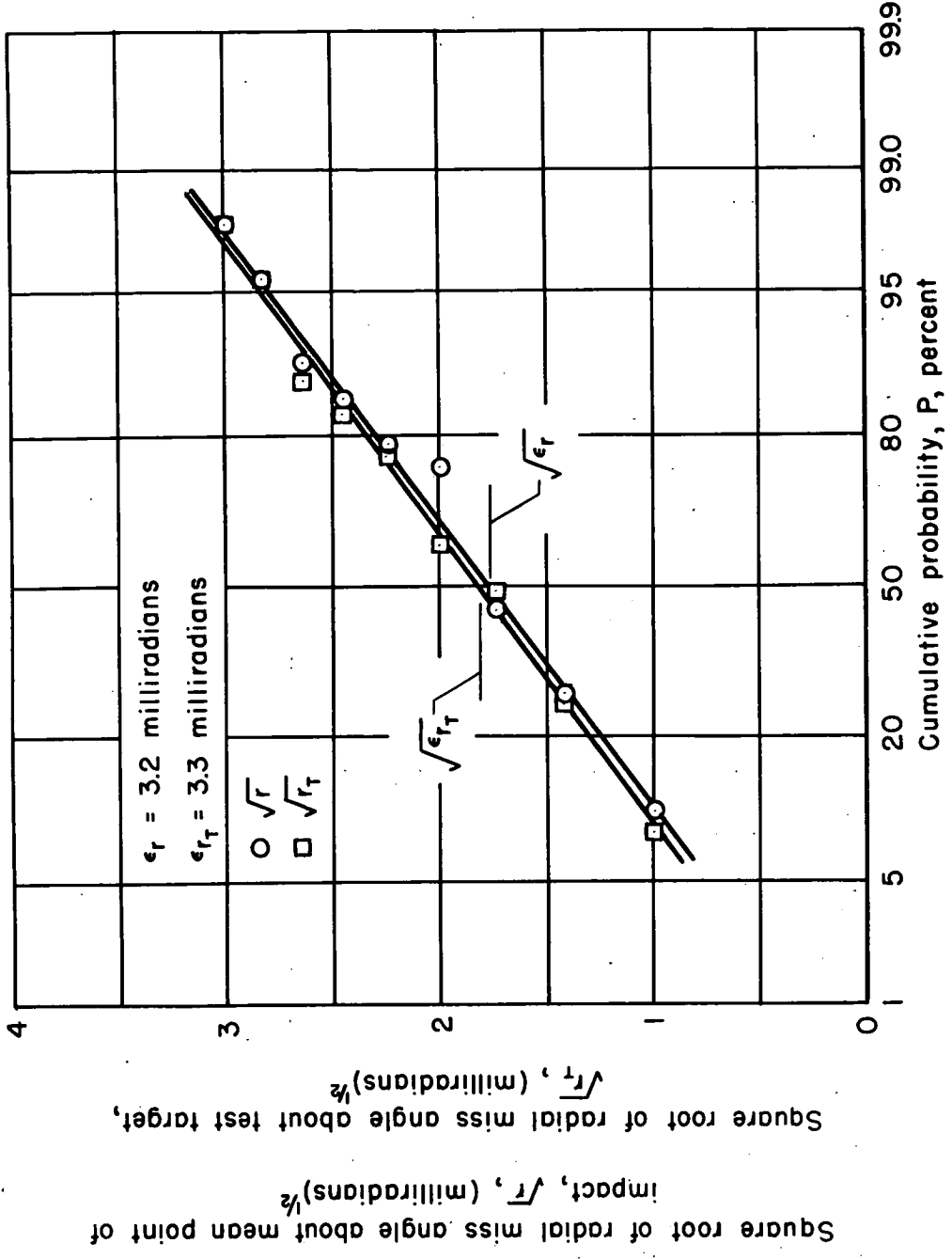


Figure 17.- Cumulative probability distribution of the radial miss angle; 15,000-foot firing range, with initial dispersion.



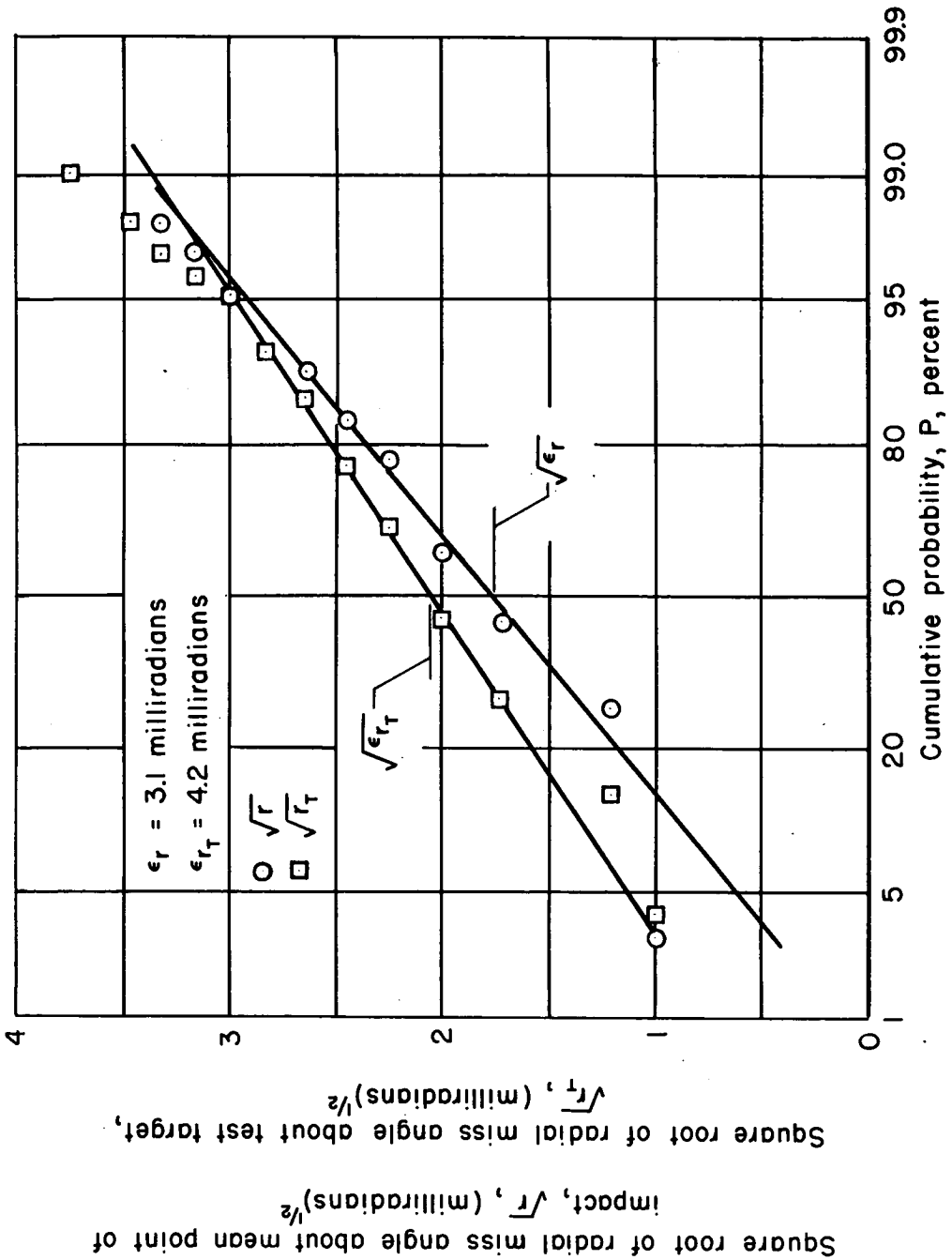


Figure 18.- Cumulative probability distribution of the radial miss angle; 8,000-foot firing range, no initial dispersion.

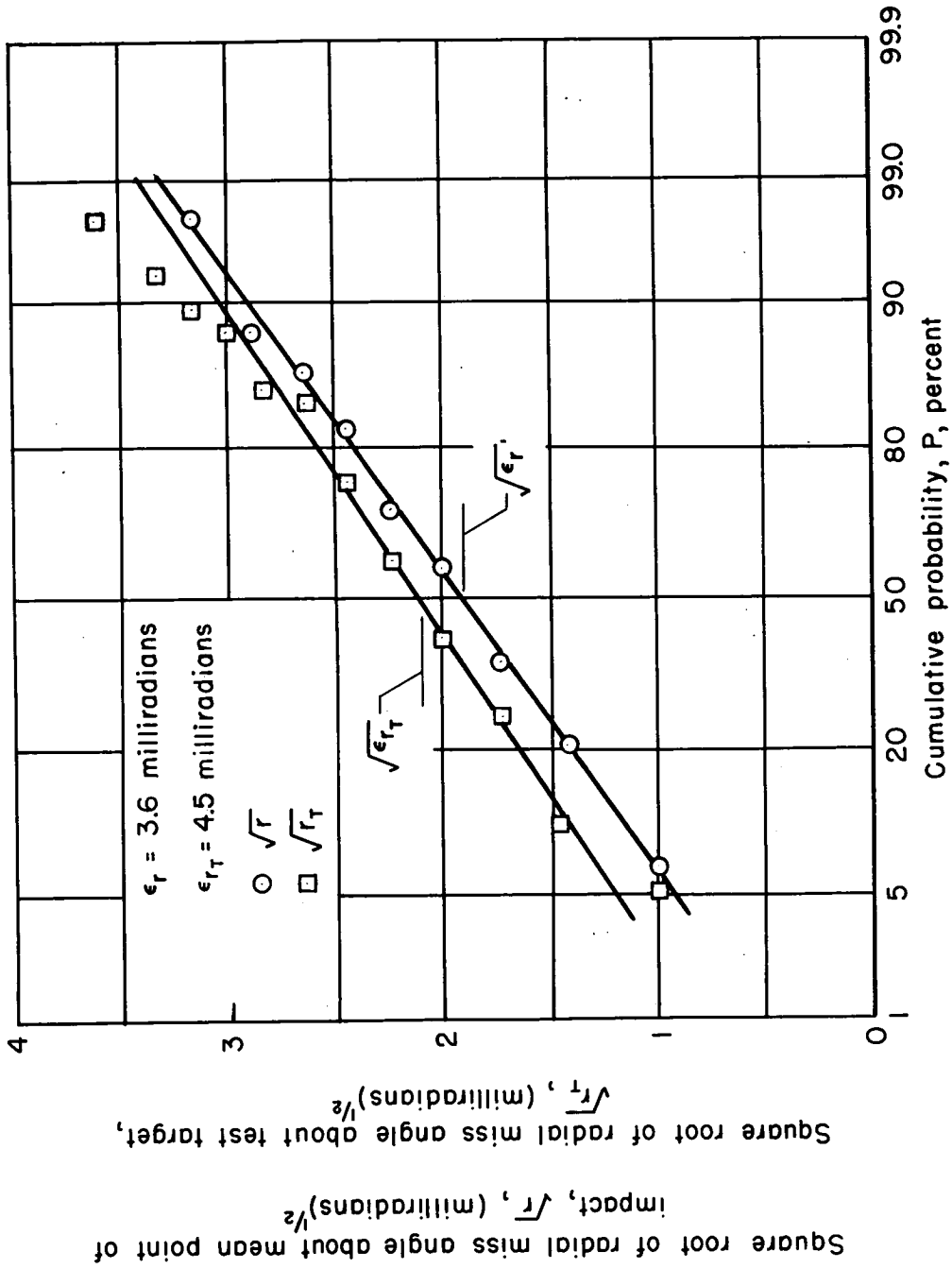
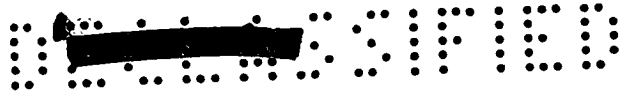


Figure 19.- Cumulative probability distribution of the radial miss angle; 8,000-foot firing range, with initial dispersion.



[REDACTED]

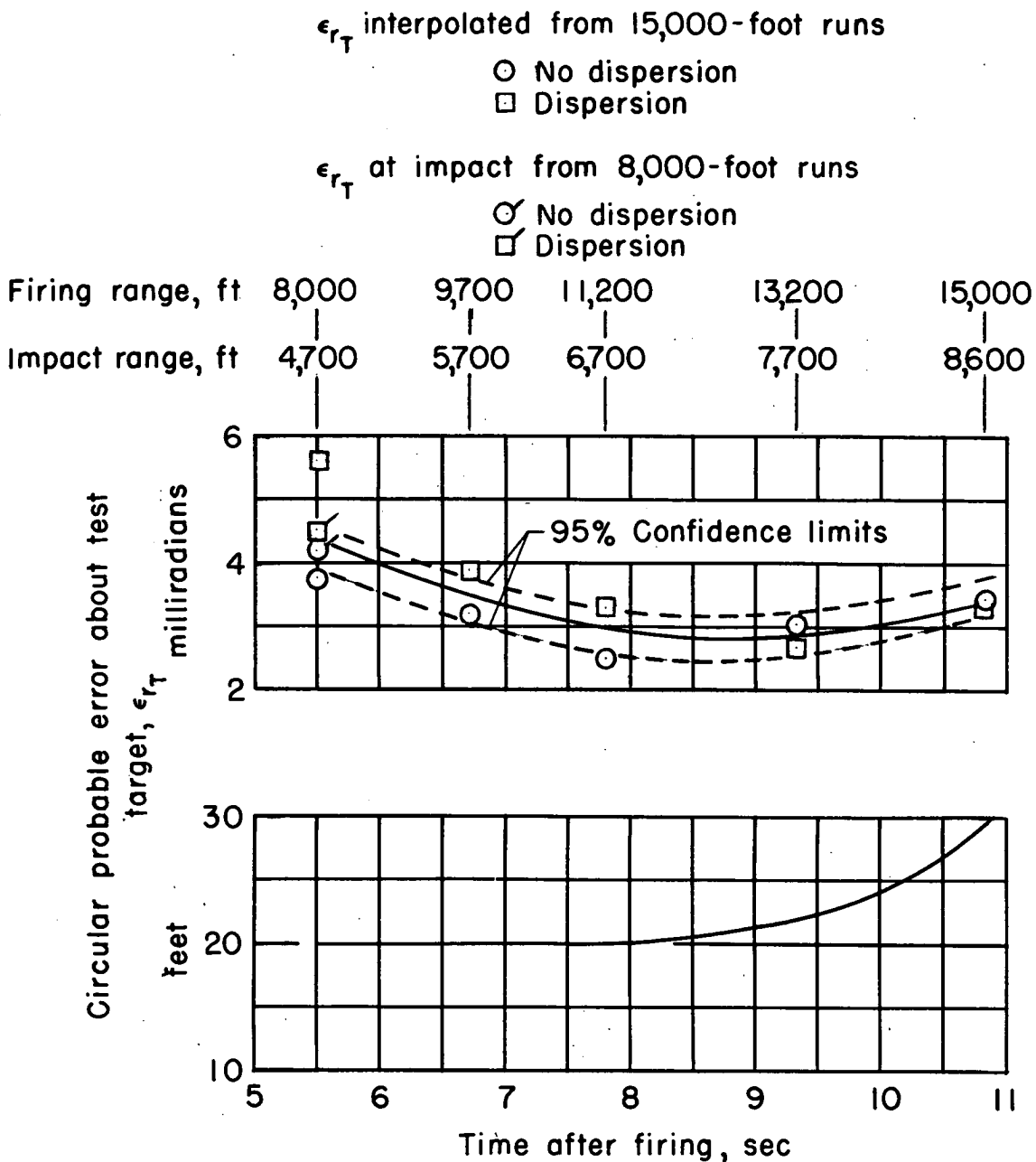
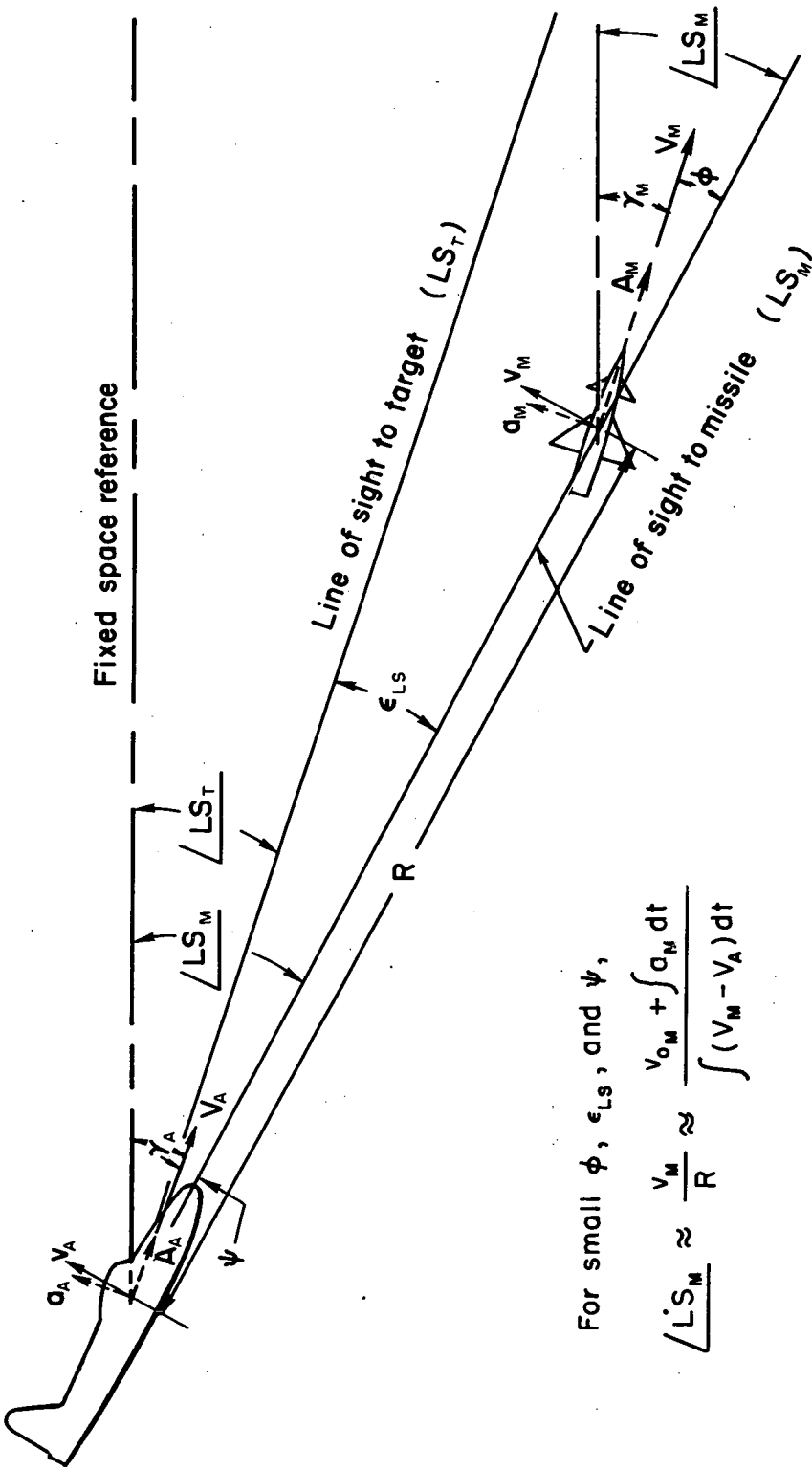
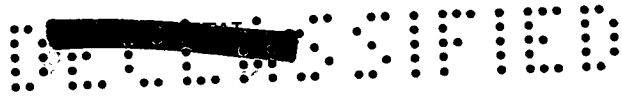


Figure 20.- Variation of circular probable error with missile time of flight.

[REDACTED]



For small ϕ , ϵ_{LS} , and ψ ,

$$\delta LS_M \approx \frac{V_M}{R} \approx \frac{V_{0M} + \int a_M dt}{\int (V_M - V_A) dt}$$

Figure 21.- Geometry of the missile simulation problem.



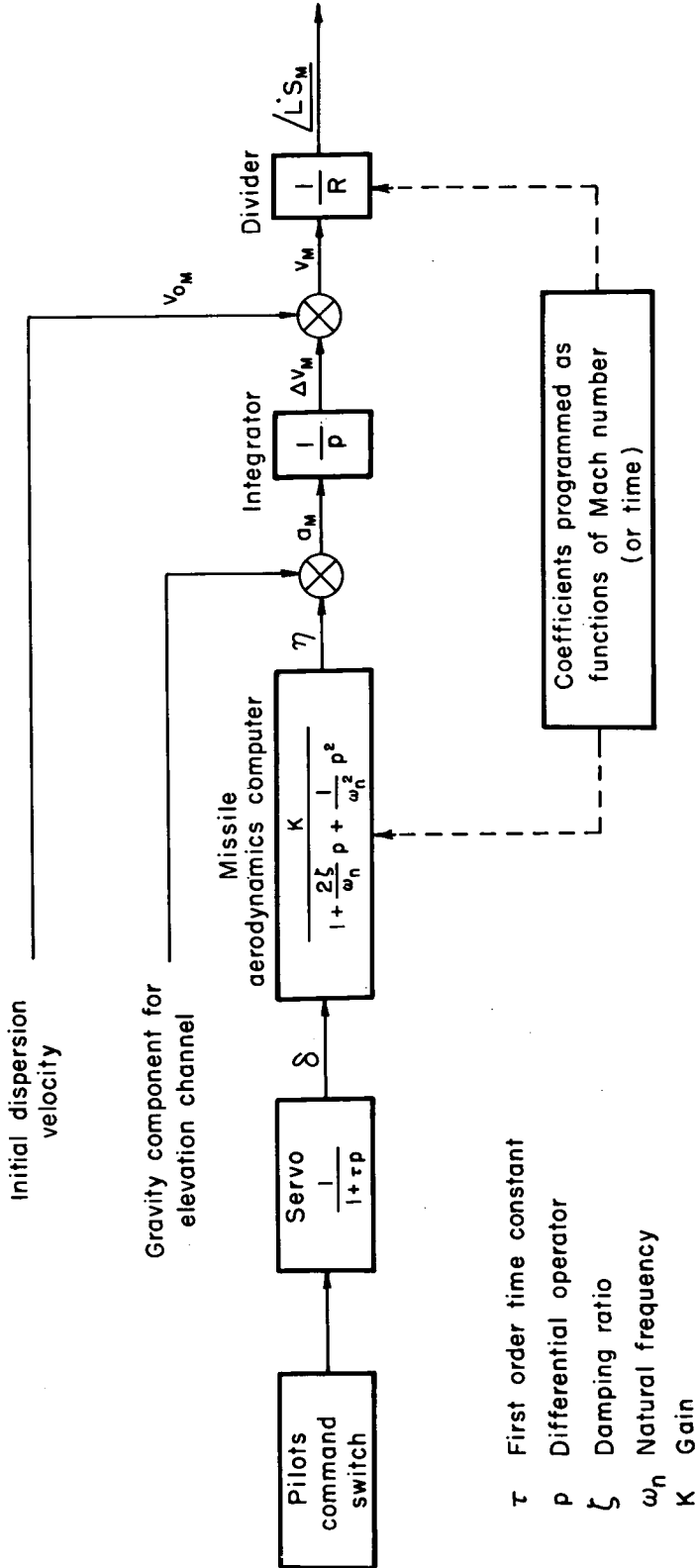
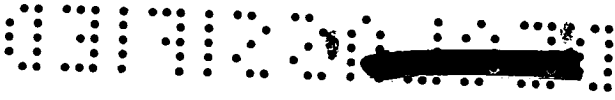


Figure 22.- Block diagram of one channel of a conventional analog computer for a missile simulator.

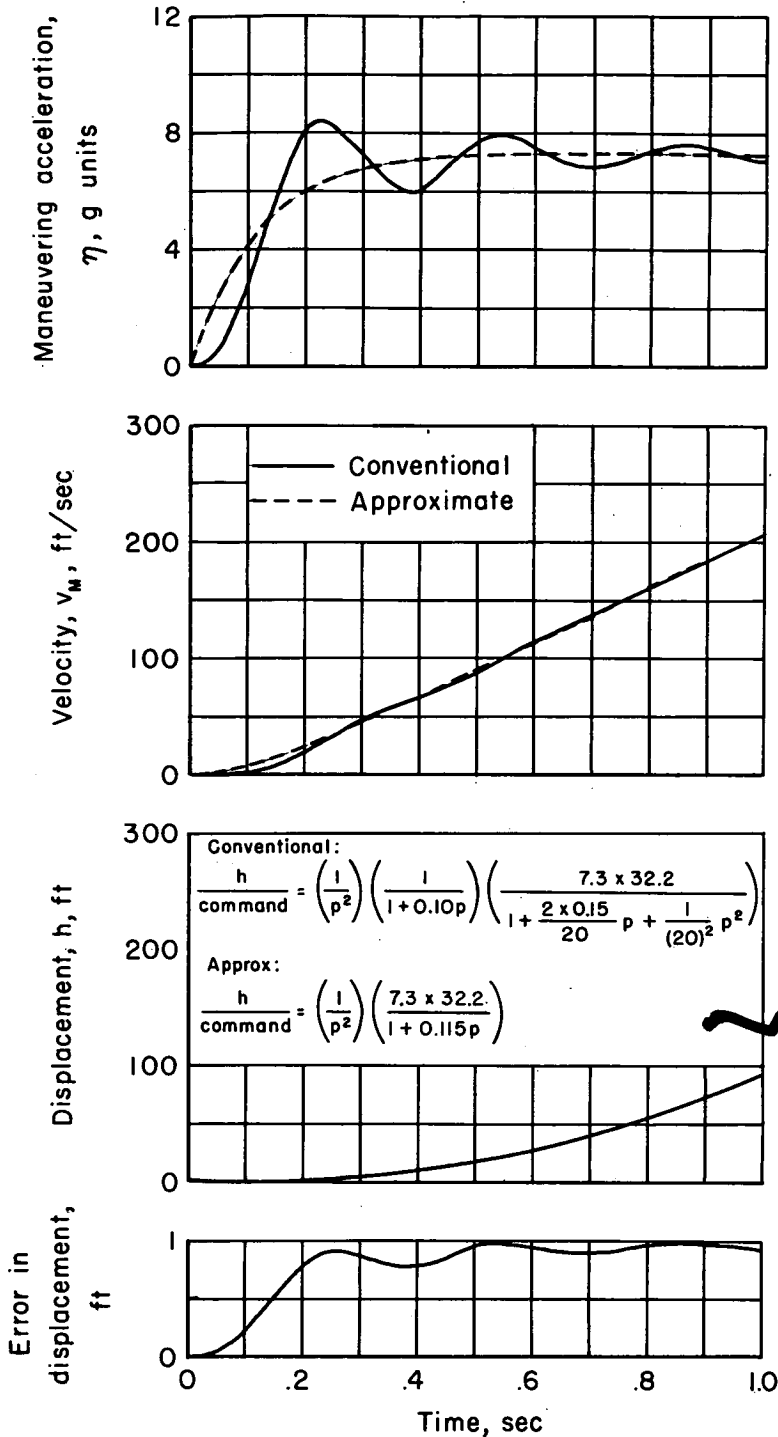


Figure 23.- Comparison of response to step command of conventional and approximate missile analogs.

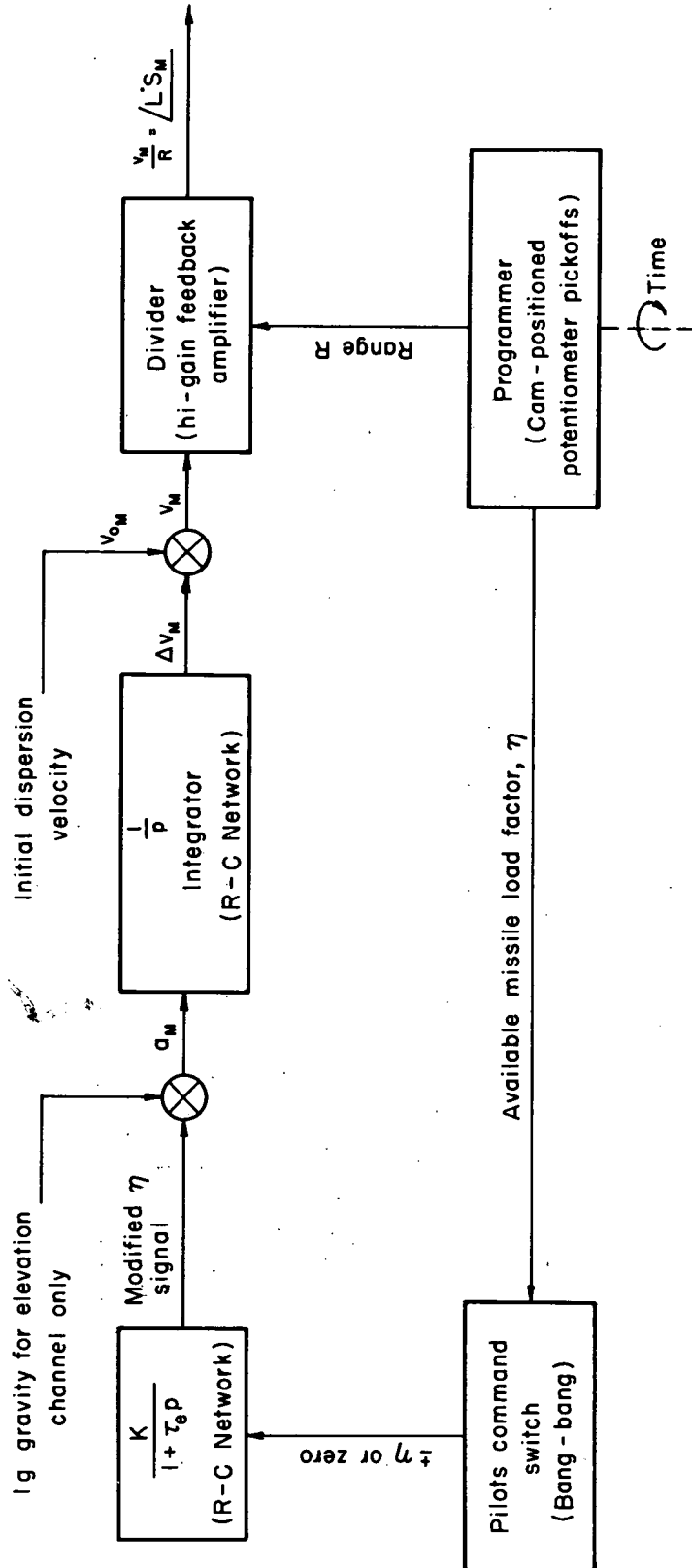


Figure 24.- Simplified block diagram of one channel of Ames airborne missile analog computer.

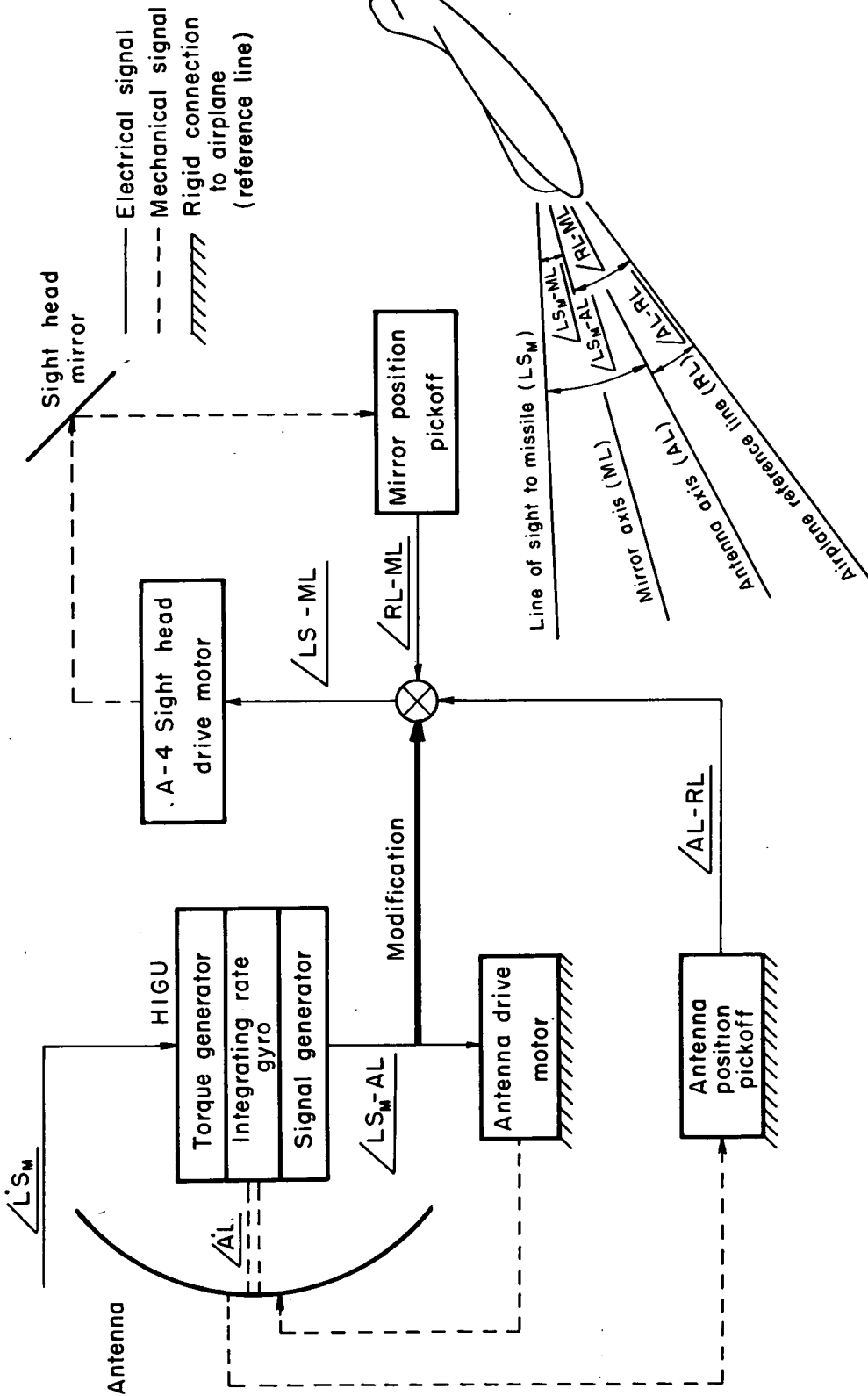


Figure 25.- Block diagram of airborne missile simulator space-stabilization and sight-head mirror drive loops.

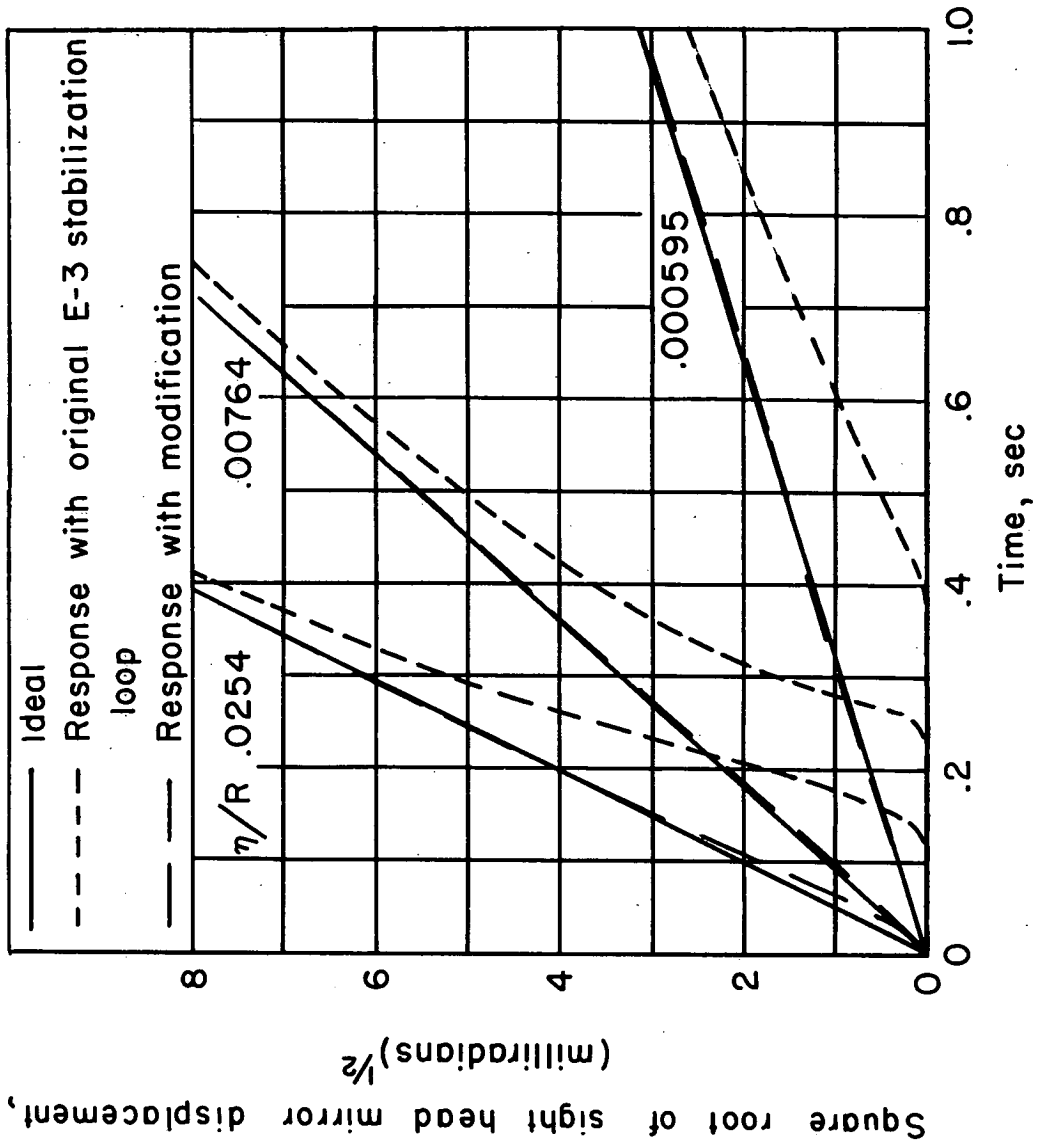
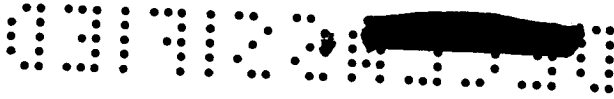


Figure 26.- Response of missile dot to step acceleration command.

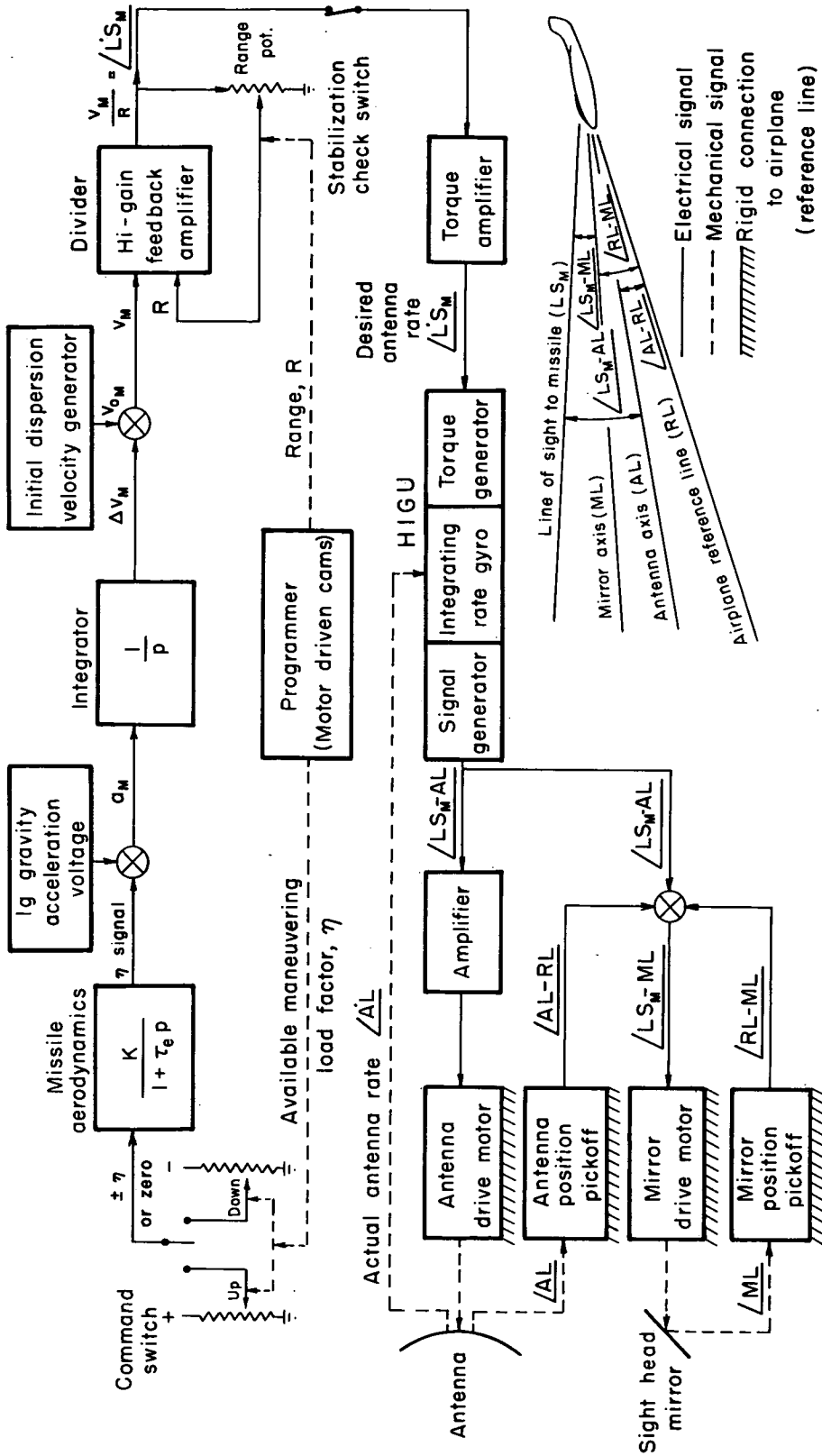


Figure 27.- Block diagram of elevation channel of missile simulator as installed in test airplane.

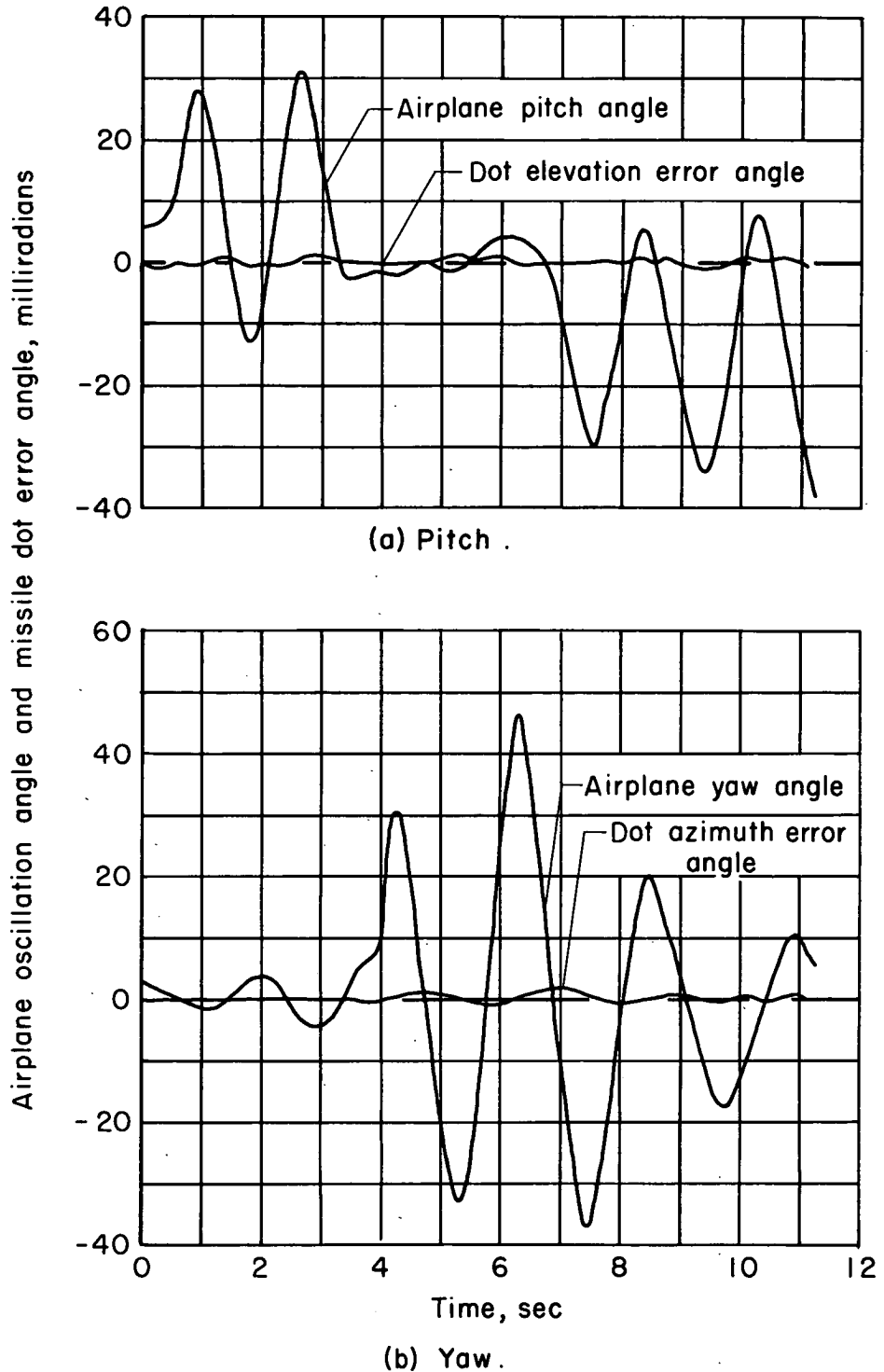
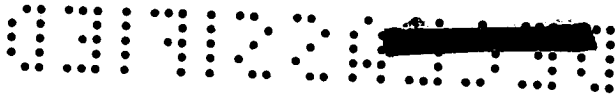


Figure 28.- Stabilization of missile dot during oscillations at airplane natural frequency.

A motion-picture film supplement, carrying the same classification as the report, is available on loan.

The film (16mm., 10 min., color, silent) shows the following sequences: runs demonstrating the stabilization of the missile dot against airplane oscillations, runs typical of simulated Bullpup attacks against the test target, and simulated attacks against airplane and ground targets.

The film may be borrowed on application to the

Chief, Division of Research Information
National Advisory Committee for Aeronautics
1512 H Street, N. W.
Washington 25, D. C.

Requests will be filled in the order received. You will be notified of the approximate date scheduled.

NOTE: It will expedite the handling of requests for this classified film if application for the loan is made by the individual to whom this copy of the report was issued. In line with established policy, classified material is sent only to previously designated individuals. Your cooperation in this regard will be appreciated.

Date _____

Please send, on loan, a copy of film supplement to RM A56G24

Company name

Street number

City and State

Attention: Mr. _____

(To whom copy No. _____ of RM was issued)

037122A.030

Place
stamp
here

Chief, Division of Research Information
National Advisory Committee for Aeronautics
1512 H Street, N. W.
Washington 25, D. C.

CONFIDENTIAL

03 910 20 1030

CONFIDENTIAL